Dissertation
on

Modelling, Control and Experimentation for Vibration Suppression of Single Link Flexible Manipulator

Submitted in partial fulfilment of
Requirements for the degree of

Master in Engineering
in
CAD/CAM
by

Ebin Mathew
801784005

under the supervisions of

Dr. Tarun Kumar Bera
Associate Professor

Dr. Ashish Singla
Associate Professor

Department of Mechanical Engineering
TIET

Department of Mechanical Engineering
Thapar Institute of Engineering & Technology
(Deemed to be University)
Patiala-147004, Punjab
July, 2019

DECLARATION

*I hereby declare that the work done in thesis report entitled, "***Modelling, Control and Experimentation for Vibration Suppression of Single Link Flexible Manipulator***" submitted towards partial fulfilment of award of* ***Master of Engineering degree*** *in* ***CAD/CAM Engineering*** *in* ***Department of Mechanical Engineering*** *of* ***Thapar Institute of Engineering and Technology, Patiala*** *is an authentic record of work carried out by me under the supervision and guidance of* ***Dr. Tarun Kumar Bera and Dr. Ashish Singla, Associate Professor, Mechanical Engineering Department*** *of* ***Thapar Institute*** *of* ***Engineering and Technology, Patiala.***

Date: 30/7/2019

Ebin Mathew

This is to certify that above declaration made by the student concerned is correct to the best of our knowledge and belief.

Tarun Kumar Bera 30/7/19

Dr. Tarun Kumar Bera

30/7/19

Dr. Ashish Singla

Associate Professor
Department of Mechanical Engineering
Thapar Institute of Engineering & Technology
(Deemed to be University)
Patiala – 147001, India
tkbera@thapar.edu ashish.singla@thapar.edu

Acknowledgement

It is my great fortune to get an opportunity to work on this challenging yet inspiring project. The learning and experience I have received here is of inexplicable value. It gives me immense pleasure to express my paramount gratitude to each one of those who made this possible.

It has been my immense pleasure to complete this project under the guidance of two renowned expertises. I would start by expressing my profound exaltation and gratitude to Dr. Tarun Kumar Bera, Associate Professor, Department of Mechanical Engineering, Thapar Institute of Engineering and Technology for sharing his priceless experience in the field of modelling and simulation. I will owe him a life time for not only helping me learn a new modelling technique to develop system dynamics but also for helping me selflessly in the project. I thank him from the core of my heart for standing by me through all highs and lows of the process and at times steering the research in right direction for me to achieve my objectives. He will always be my ideal of discipline and optimism.

Next, I would like to thank Dr. Ashish Singla, Associate Professor, Department of Mechanical Engineering, Thapar Institute of Engineering and Technology for considering me and giving me a chance to be part of this DST project. His impeccable knowledge in the field of robotics and control has helped me in achieving my goals. I sincerely thank him for introducing me to the field of robotics and control by teaching me all the basics required and giving hands on experience on real life systems.

Also, I would like to heartily convey my gratitude to Thapar Institute of Engineering and Technology, Patiala, for providing me with the lab facilities for my research.

Finally, I would like to thank five of my close friends namely Suraj, Ashwin, Rajat, Jonty and Veronica also, my senior colleague Prakhar Jain for directly or indirectly helping me complete my project and motivating me through tough times.

Ebin Mathew

Abstract

The use of robotic arms in various sectors has been increased over a decade. Attempts to improve their performance and design are being made since many years. The size and weight of these arms have been a matter of concern in their design and application. By reducing the cross-sectional area, the weight of the arm reduces considerably but, the rigidity of the arm has to be compromised since the workspace of the arm cannot be altered. Many researchers have suggested various methods to develop these flexible robotic arms. Due to the non-linearity of the system and the complexity of deriving a solution, only discrete forms of modelling like FEM, lumped parameter method, assumed mode method have gained worldwide recognition. Some of these methods do not produce accurate results even for single arm manipulator system while others produce inaccurate results when the number of arms increases. Therefore, a suitable mathematical technique is yet to be developed which will produce accurate results. A rotary flexible link has been modelled in the present work using a conventional method of modelling (lumped parameter model) and is compared with the Rayleigh beam model developed considering the rotary inertia acting on the flexible link. The Rayleigh beam model is developed using bond graph notation. Both the models are validated with experimental results of rotary flexible link. Modern control theories have been discussed and applied on both the dynamic models. The results obtained are compared with experimentation and final conclusion has been stated in detail. Adequate results have been obtained from the Rayleigh beam theory. This model can be refined further for more accuracy. The model can be extended for multi-link flexible manipulators.

Keywords: Flexible link, Discrete form, Rayleigh beam theory, Bond graph, Linear quadratic regulator, Experimentation

Nomenclature

e_{ss}	Steady state error
g	Acceleration due to gravity
Δh	Change in height
J_{eqv}	Mass moment inertia of hub
J_l	Mass moment inertia of link
J_s	Mass moment of inertia of flexible link
K	Translational kinetic energy
K_g	Gear ratio
K_{gn}	Product of gear ratio and gear box efficiency
k_m	Back-emf constant
K_s	Flexible link stiffness
K_{Total}	Total kinetic energy
k_t	Motor torque constant
L	Total length of flexible link
m	Mass of flexible link
n_g	Gear box efficiency
n_m	Motor efficiency
P_e	Elastic potential energy
P_g	Gravitational potential energy
P_o	Percent overshoot
P_{Total}	Total potential energy
R_{eqv}	Viscous friction coefficient

R_{m}	Motor armature resistance
t_{s}	Settling time
u	Control input
V_{m}	Voltage
x	State variable
α	Angle of deflection
α_{m}	Maximum angle of deflection
θ	Angle rotated by hub
λ	Eigen value
τ	Motor torque
ω	Natural frequency
ω_{R}	Natural frequency of Rayleigh beam model

List of Abbreviations

FEM	Finite element method
LQR	Linear quadratic regulator
PD	Proportional derivative
SE	Source of effort
SF	Source of flow
TF	Transformer
GY	Gyrator
	Rayleigh beam element/capsule

List of Figures

List of Tables

Table of Content

Chapter 1 Introduction

Automation has increased on a very large scale in many sectors like production industries, medical surgeries, nuclear power plants *etc*. Human labour has been replaced with robotic arms for various operations. The conventional arms which are used in industries for production lines require having accurate positioning with negligible vibration. For obtaining this, the robotic arms are made of high stiffness materials and are given larger cross sectional areas. Therefore, these manipulator arms are heavy in weight. Following problems are caused due to the use of heavy arms, they consume more power from the source for their functioning, requires bigger size of actuators, heavy nature causes hindrance in transportation *etc*. If the cross sectional area of these arms are reduced without changing their length to maintain the same workspace, these arms become flexible in nature because bending can easily occur. The use of flexible arms started in space applications where robotic arms need to be light in weight as well as should be of high performance in terms of positional accuracy, speed, reduced vibrations *etc*. Over the time, attempts are being made to use flexible arms in other sectors also.

Apart from performance point of view, these heavy rigid arms can also prove to be more dangerous and destructive during malfunctioning. A slight error in control can be hazardous on the shop floor. On the other hand, flexible manipulators have more advantages compared to the conventional rigid and heavy arms in terms of performance as well as safety. Flexible arms are lighter in weight and hence, it will require less power to move at the same speed of the conventional rigid arms. This in turn reduces the size of the actuators to be used to drive the arm reducing the cost of the system to be used in production.

However, the use of flexible arms has not gained much favour in industries as bending and vibrations are induced in these arms during their working. These vibrations in the arms need to be controlled in order to achieve positional accuracy. If an accurate and easy technique of modelling, designing and controlling a flexible arm is developed, it will open its door to many other applications in industries *e.g*. spray painting, robotic arm welding *etc*. On a wider scale apart from the industrial application, they can also be used for medical surgeries. This will in turn help to reduce labour and will give push to automation in many other sectors. This Thesis-work is a step to find new method for

modelling and controlling the end point vibration of a flexible arm manipulator using Rayleigh beam theory with bond graph technique. It will be focused on developing this method to be more accurate and simpler compared to the previous methods which has been used to develop the dynamic model and control of a flexible arm.

1.1 Background and Motivation

Over the years, automation has given a boost to the development of robotic arms in many applications, from industrial use to medical appliances. These automated arms are being used on a very large scale. But, apart from lowering the cost of making these robotic arms, the primary goal in designing them is to increase their precision and accuracy in placing objects at the desired location, to increase their response time for a given input and to lower its energy consumption. Many researches have been done to develop an optimum mathematical model which can be used to design these arms. These mathematical models will not only help to predict the motion of the arm, the vibration produced in them, the time taken by them to give a steady response, understand the arms behaviour on various loading conditions but, will also help to understand the major factors that has to be considered while making an actual working model of a flexible arm. These mathematical models will form the basis of design and development of flexile manipulators. As it has been already mentioned that the use of flexible manipulator can be applied in numerous number of application, it is necessary to have an efficient as well as simple method of modelling and controlling them. Discrete methods like finite element method, assumed mode method, lumped parameter method have been used previously for mathematical modelling of flexible arms. But, more accurate mathematical models are still to be obtained for multi-link manipulator system in order to obtain desired and faster results. In this Thesis work, Rayleigh beam method will be used to create the mathematical model and a graphical representation (bond graph technique) of dynamic model of flexible arm manipulator will be used. Bond graph of the flexible arm will be made and simulated using one of the bond graph software called SYMBOLS Shakti. In the first stage, a flexible arm will be mathematically modelled as well as the time response of various parameters will be simulated and recorded for validating it with the actual working model of flexible manipulator setup. In the second stage, various controllers will be used to control and

suppress the end point vibrations of a flexible arm. If an optimum model is developed successfully, this work can be further extended for the modelling of multi-link flexible manipulators *i.e*. two link and three link flexible manipulators.

1.2 Introduction to Flexible Link Manipulator

The size of the robotic arms cannot be reduced by reducing the length of the arm because reducing the length will reduce its workspace. Therefore, in order to make these arms lighter in weight without altering their workspace, the cross sectional area of the arms has to be reduced. If the cross sectional area of the arm reduces considerably in comparison to its length, these arms become flexible in nature. Rotational motion, payloads *etc*. can not only cause bending in the arm but also induce vibrations in them. Hence, such arms are referred as flexible arms.

1.2.1 Single Link Flexible Manipulator

A manipulator system consisting of a single flexible robotic arm is shown in Fig. 1.1. $\overline{\text{OA}}$ represents the flexible link in the rectangular co-ordinate system. If the link $\overline{\text{OA}}$ is rotated by an angle θ the flexible link deflects by an angle α due to its flexible nature. X_1 is the reference axis which is tangent to the flexible link. τ is the applied torque.

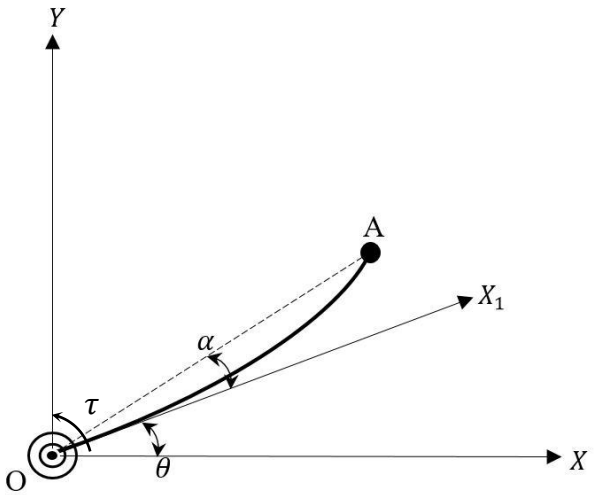

Fig. 1.1 Sketch of single link flexible manipulator

1.2.2 Two Link Flexible Manipulator

A manipulator system consisting of two flexible robotic arms are shown in Fig. 1.2. The first link is represented by $\overline{\text{OA}}$ and the second link is represented by $\overline{\text{AB}}$. If these arms are rotated by a certain angle, both the links deflect from their reference position due to their flexible nature. $\theta_1$is the angle turned by link $\overline{\text{OA}}$ and α_1 is its angle of deflection. θ_2 is the angle rotated by the link $\overline{\text{AB}}$ and α_2 is its angle of deflection. τ is the applied torque

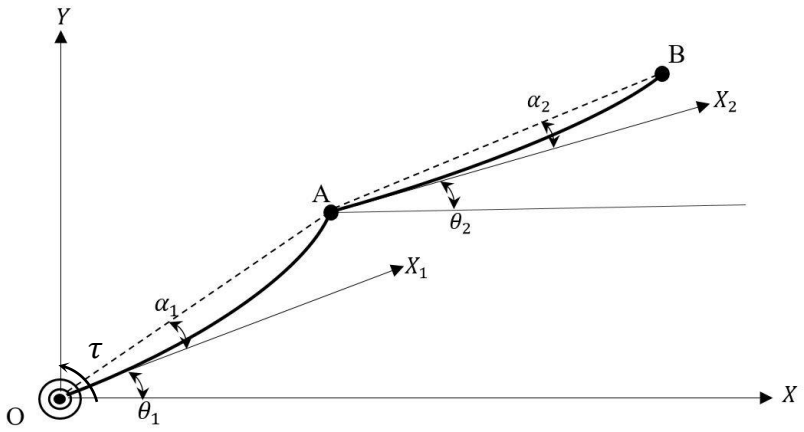

Fig. 1.2 Sketch of two-link flexible manipulator

1.2.3 Three Link Flexible Manipulator

A manipulator system consisting of three flexible robotic arms are shown in Fig. 1.3. The first link is represented by $\overline{\text{OA}}$, the second link is represented by $\overline{\text{AB}}$ and the third link is represented by $\overline{\text{BC}}$. If these arms are rotated by a certain angle, all the three links deflect from their reference position due to their flexible nature. $\theta_1$is the angle turned by link $\overline{\text{OA}}$ and α_1 is its angle of deflection. θ_2 is the angle rotated by the link $\overline{\text{AB}}$ and α_2 is its angle of deflection. θ_3 is the angle rotated by the link $\overline{\text{BC}}$ and α_3 is its angle of deflection. τ is the applied torque

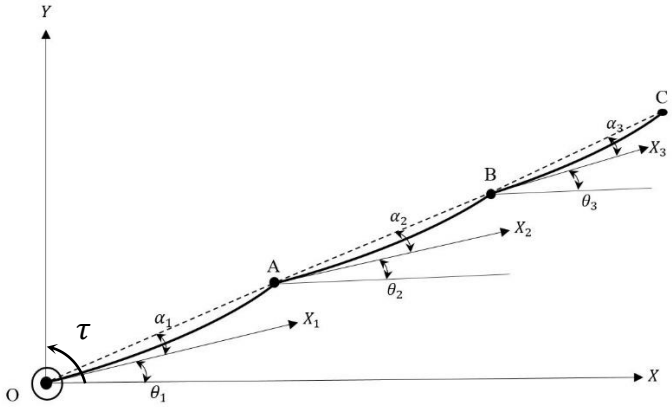

Fig. 1.3 Sketch of three-link flexible manipulator

1.3 Comparison between Conventional and Flexible Robotic Arm

If a workspace is assumed, the conventional robotic arms will have a larger cross sectional area compared to the flexible robotic arm. Thus the conventional arms will be heavier and more rigid compared to the later counterpart. The energy and the size of the actuators required to move the conventional arm will be more. The portability of these arms will be less than a flexible robotic arm which will be lighter in weight. During malfunction these conventional robotic arms can create a more fatal environment around them. But, the conventional arms are quite better if, bending and end point vibrations of arm are considered. If these drawbacks of the robotic arms are solved, development of very light weight highly optimise robotic manipulators will be possible in future.

1.4 End Point Vibration Suppression of Flexible Manipulator

This section of the chapter states the difficulties in making robotic arms lighter in weight by reducing their cross sectional area. The difficulties in modelling the dynamic models of such system are also stated in the following sub-section.

1.4.1 Need of Vibration Suppression

The flexible nature of robotic arms can cause various unwanted noise in the system output *e.g.* when a flexible arm is rotated by a certain angle vibrations are induced in the arm when it stops. This is because the robotic arm is long in its length but the cross sectional area of the arm is comparatively very small. This induces the flexible nature

and it has to be addressed. The end point vibrations will cause inaccuracy when the arm will try to displace an object, these vibrations can be hazardous if used as a medical surgery robotic arm, in welding these vibrations will weld the undesired areas, *etc*. Every sector using flexible robotic arms will face undesired outputs if its vibrations are not controlled.

1.4.2 Challenges in End Point Vibration Suppression

In order to design and manufacture a robotic manipulator, the behaviour of the system should be known prior. A mathematical model of the system will help in knowing how the system responds for various inputs and system conditions. With the help of this, the system design parameters can be altered according to the user requirements. Modelling a robotic arm mathematically considering all the design parameters which will be used, will help to know which control theory can be used for vibration suppression. When a flexible arm is modelled mathematically, a highly non-linear system with infinite degrees of freedom is developed. This system is not only difficult to model but, application of control theories on such systems is also difficult and expensive. The control torque can be provided only at the joints of the arm and not elsewhere. The numbers of sensors used to measure the states of the system are also limited. Hence, various assumptions are to be made while developing the dynamic model of a flexible arm. The challenge is to develop a mathematical model which can accurately predict the behaviour of an actual flexible arm and apply a control theory which can help in suppressing the vibrations that are induced in the arm when they are rotated through a certain angle.

1.5 Research Methodology

In the present work a dynamic model of a robotic manipulator consisting of a flexible arm is developed with an aim that, the behaviour of an actual flexible arm will be predicted accurately using this dynamic model. This will help in design and development of flexible arm robotic systems. Figure 1.4 shows a schema diagram which represents the outline of the research carried out in this thesis. A flexible manipulator has two stages of its development. They are; the modelling method used to develop the dynamic model and the control technique applied on the dynamic model

in order to achieve the desired working of the arm. The present work is based upon minimizing the vibrations that are induced in the arm and also minimizing the steady state error of the actuator for a given input *e.g.* the motor which will rotate the arm should trace the exact desired angle specified by the user. Therefore, the outputs that have been measured from the dynamic models are the hub angle of rotation *i.e.* angle turned by the motor which rotates the arm and the deflection of the tip of the arm from its reference position. The left side of the diagram shows that two methods are used to develop the mathematical model of a flexible arm. The first method is the lumped parameter method. Using this method, a lumped model of a manipulator system is developed and with the help of Euler-Lagrange method the dynamics of the system is developed. The state space representation of the system is developed and using MATLAB along with Simulink simulations are carried out and the outputs are recorded. The second method used to develop the dynamic system is the Rayleigh beam theory. This dynamic model has been completely developed using bond graph approach. SYMBOLS Shakti is the modelling and simulation software used to record the outputs of the dynamic model. In the later stage, an experimental setup is used to compare the theoretical results which the actual working of a flexible link. A detailed comparison about the performance of each model and their time domain response has been made in Chapter 3 and Chapter 4. The right side of the diagram shows how the control theories have been applied on the dynamic models developed. Two controllers have been used for this purpose; full state feedback control and linear quadratic regulator (LQR). The LQR gains generated for the lumped parameter model has also been implemented on the actual setup and the results obtained are compared with the theoretically controlled models. The detailed comparisons of all the performance parameters have been made in Chapter 5.

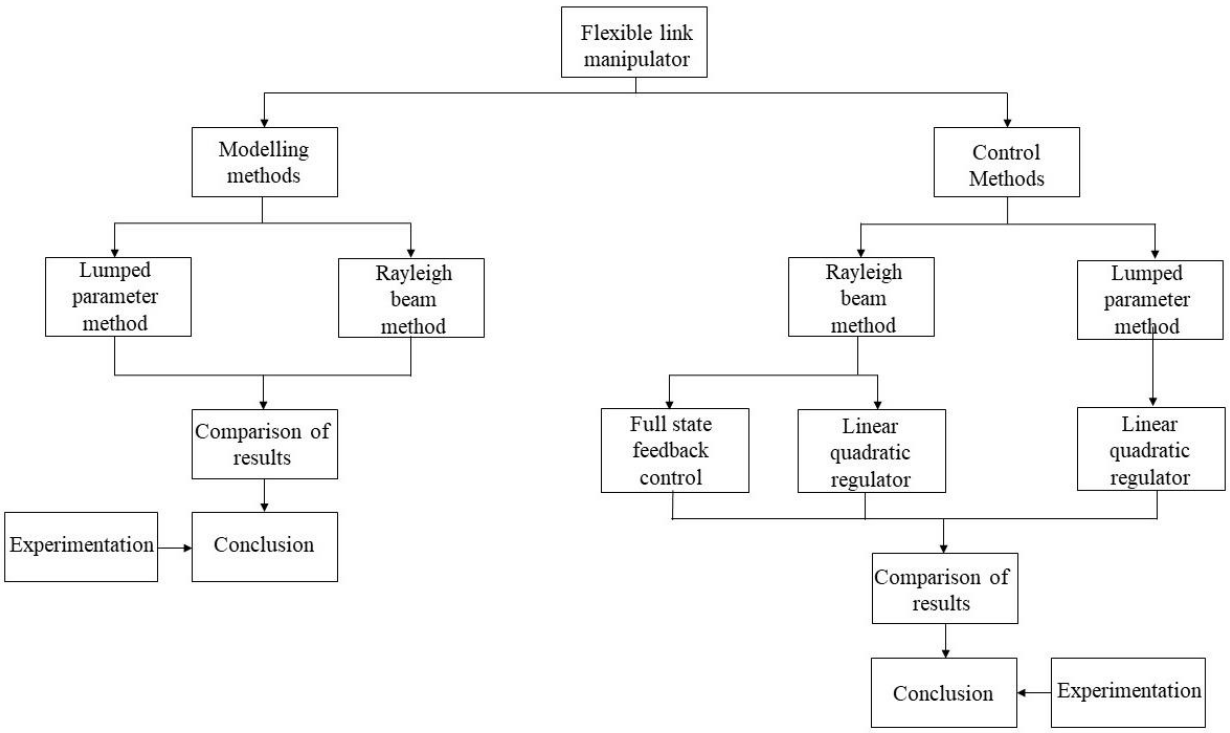

Fig. 1.4 Flow chart of Research Methodology

1.6 Bond Graph Approach

Bond graph is a structural representation of any system in a graphical form. It allows transfer of energy between the sub systems of similar or dissimilar energy domain without losing its topology. This tool for developing and solving the dynamics of a system was developed in the year 1959 by Prof. H.M. Paynter. He connected the elements of a system using power bonds. The unique characteristic of bond graph is the bi-directional flow of information (flow and effort) which takes place between the junctions. There are seven basic elements that are used in bond graph to model a system. The seven elements are; inertial (I), compliance (C), dissipater (R), source of effort (SE), source of flow (SF), transformer (TF) and gyrator (GY). Using these seven elements any system can be modelled. To develop the bond graph representation of any system the effort and flow variables should be recognized. The flow and effort variable for different energy system are shown in Table 1.1.

Table 1.1 Effort and flow variables in various energy domain

System	Flow (e)	Effort (f)
Electrical	Current	Voltage
Hydraulic	Volume flow rate	Pressure
Chemical	Molar flow rate	Chemical potential
	Mass flow rate	Enthalpy
Magnetic	Magnetic Flux	Magneto-motive force
Thermal	Entropy flow rate	Temperature
	Volume flow rate	Pressure
Mechanical	Velocity	Force
	Angular Velocity	Torque

1.6.1 Different Elements of Bond Graph

The basic single port elements required to model a system using bond graph notation are discussed in this section.

Resistive element: This element is represented by 'R' in bond graph. The resistive element is analogues in all the energy domains. The resistors used in an electrical system, damper and dashpots used in mechanical system, porous plugs in fluid system, *etc*. comes under this category. The causality of this element can be resistive or inductive. Figure 1.5 (a) shows the graphical representation of a resistive element.

Compliance element: This is an energy storing element and is represented by 'C'. An accumulator in hydraulic system, a capacitor in electrical system, a spring in mechanical system, *etc*. are represented by this element. An algebraic relation is formed between effort and generalized displacement. It also forms a relation between effort and time integral of flow. Figure 1.5 (b) shows a mechanical spring having a stiffness *K* using bond graph representation.

Inertial element: This element stores energy and is represented by 'I'. This element forms a relation between flow and time integral of flow. In mechanical system inertial elements, inductance in electrical system, *etc*. are represented using this element. An inertial element with mass *m* is shown in Fig. 1.5 (c).

Source of effort: This element represents an active port in the system and is denoted by 'SE'. The half arrow is never towards the port *i.e.* the half arrow will always be facing away from the port since this port is used when an external effort is shown on the system. In hydraulic system the pressure acting on the system, torque and force in

the mechanical system, voltage in electrical system, *etc*. are represented by this element. The graphical representation of an effort source is shown in Fig. 1.5 (d).

Source of flow: This element is used when a power input is given to a system in form of flow. This element is represented by 'SF'. In mechanical system displacement, volume flow rate in hydraulic domain, current in electrical systems, *etc*. are represented using this element. Figure 1.5 (e) shows the graphical representation of flow input element.

Transformer: This is a two port element. A transformer in electrical system, a mass-less lever in mechanical system *etc*. are represented by this element. This element does not produce energy neither it consumes or destroys energy. This element is used to convert one form of energy to another form of energy or can be used as a scalar multiplier which will help to magnify or reduce the input from one side of the element to the other. The modulus (μ) of the element is the multiplication factor. It is denoted by 'TF'. Figure 1.5 (f) shows the graphical representation of a transformer element.

Gyrator: This element helps to convert effort to flow or vice versa. A DC motor in electrical system, a gyroscope in mechanical system *etc*. are represented by using this element. A gyrator is denoted by 'GY'. Figure 1.5 (g) shows the graphical representation of a gyrator element.

0-junction: This junction follows the Kirchhoff's law or the analogy used in plumbing that, the flow that leaves from a junction must to the flow that is input to the junction. The number of bonds connected to this point depends on the system being modelled. The direction of the half arrow shows the direction of the flow. A LCR circuit in parallel can easily define the use of '0' junction. Figure 1.5 (h) shows a LCR circuit in parallel connection and Fig. 1.5 (i) shows its graphical representation using bond graph.

1-junction: This element follows the mesh law which says that, the summation of efforts at a junction is equal to zero. Half arrow direction decides the sign of the flow. It can be easily explained by a LCR circuit in series. Figure 1.5 (j) shows a series arrangement of an LCR circuit and Fig. 1.5 (k) shows its graphical representation using bond graph.

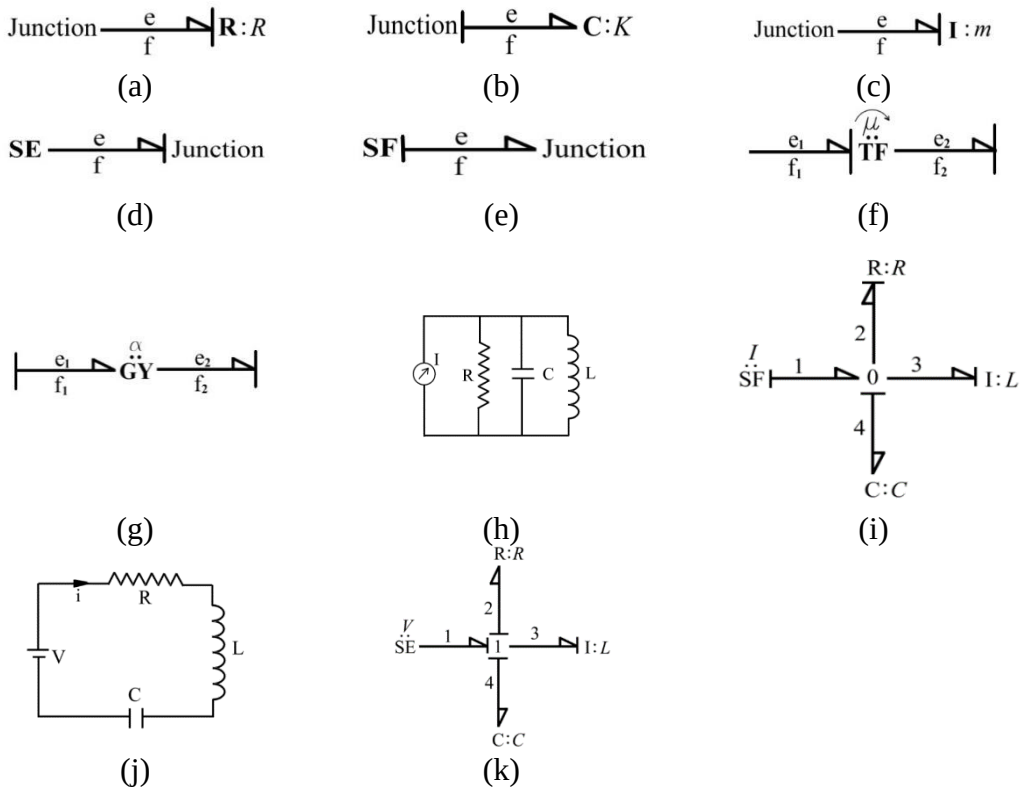

Fig. 1.5 Bond graph representation of (a) Resistive element, (b) Compliance element, (c) Inertial element, (d) Source of effort element, (e) Source of flow element, (f) Transformer element, (g) Gyrator element, (h) LCR in parallel circuit, (i) LCR in parallel, (j) LCR in series circuit, (k) LCR in series

1.7 Contribution of the Thesis

This present work gives a detailed review about the majorly used modelling techniques to develop flexible arm robotic system. All the methods that have been listed come under the discrete form of modelling. At the initial stage, a conventional method of modelling namely lumped parameter method is used to develop a dynamic model of a rotary flexible link. Next, the Rayleigh beam theory which considers the rotary effect acting on the arm is used to develop for the same rotary flexible link. Chapter 3 shows the detailed modelling of flexible link using Rayleigh beam theory along with the simulation results and conclusions. Later both models are validated with the working of an flexible manipulator setup in Chapter 4. The results of all the simulations and tests are discussed in the respective chapters and appropriate conclusions are drawn. The Rayleigh beam model is yet on its initial stage of development and can be refined further for better results. Since, bond graph has been used as a tool for modelling the

given system, it makes development of this model easy and faster than the other methods. This model on further refinement can be extended to multi-link systems. This research theoretically proves that the Rayleigh beam theory is a better method to model flexible links than the conventional lumped parameter method. In the final stage, different linear controllers are applied on both the dynamic models developed. Basic modern controller like full state feedback control has been discussed and applied on the Rayleigh beam model. Though satisfactory results are obtained, the pros and cons of this controller have been explained in detail and the need for LQR control is expressed. A Rayleigh beam model based upon LQR control theory has been developed with satisfactory output results. LQR control on flexible link using lumped model is also shown. Both the controlled models are validated with an experimental setup and appropriate conclusions have been made. The scope of future work is also stated at the end.

1.8 Organization of the Thesis

The structure of the work that has been done in this thesis is as follows:

Chapter 1: It contains introduction to robotic manipulator system with flexible arms. The reason why robotic arms become flexible in nature, the use and advantages of such flexible arm robots over the conventional rigid and bulky robotic arms have been explained. Why vibrations are induced in the flexible arms and the reasons to suppress these vibrations has also been addressed. Introduction to the basics of bond graph has been given. The research methodology followed has been shown and discussed in detail. The contribution of this thesis is also stated.

Chapter 2: A detailed literature review about the various discrete forms of modelling a flexible manipulator is given in this chapter. The control techniques used on these methods are also discussed. The work that has been done and is presently going on in India has been mentioned. Literature review on bond graph modelling for flexible links and bond graph applications in various other systems is given. An attempt has been made to show the versatility of bond graph. The observations from the literature review have been stated and the objectives of the present work are also mentioned in this chapter.

Chapter 3: In this chapter, a rotary flexible link has been modelled. This system has been modelled using two mathematical methods. The two methods used are, the lumped parameter method and the Rayleigh beam theory. Both the modelling techniques and the design parameters used are discussed and stated in this chapter. The results obtained from both models are shown and discussed in detail.

Chapter 4: In this chapter an experimental setup of rotary flexible link is used to compare the theoretical models. The description of the setup and the specifications of all the elements used to make the system have been given. The sensors used to measure the various outputs with their specifications have been stated. The working of the hardware has been explained. A detailed comparison of the outputs received from the actual hardware setup with the outputs measured from both the dynamic models has been made. Conclusions are also drawn from each observation made.

Chapter 5: This chapter states the various control theories that have been applied on the dynamic models developed using lumped parameter method and Rayleigh beam theory. The advantages of LQR over pole placement method have been discussed. The results obtained from the LQR controlled theoretical models and the LQR controlled experimental setup is compared. A detailed analysis has been stated at the end of the chapter.

Chapter 6: Based upon the results obtained and the observations made in Chapter 3-5, a conclusion has been made. The future scope of the work is also stated.

Chapter 2 Literature Survey

This section of the literature review is based on the modelling and control techniques that are being used in developing dynamic models of robotic manipulators consisting of flexible arms which are used in industries and for various other applications. The research in modelling and control of flexible manipulators started in the field of space applications [**Book, 1979; Tzou, 1989**]. The first research to study and model a flexible link manipulator was carried out in 1979 [**Book, 1979**]. Later the use of flexible manipulators started in various sectors. Flexible arms have been studied for various applications like spray painting, cleaning and inspection, drawing, micro surgical operations, pick and place operations and similar other applications.

The literature review of a flexible link manipulator can be classified into two types; based on the modelling techniques that are being used to develop a dynamic model of the manipulator system which will help in predicting the performance of the system as per the requirements of the user. The performance of the system mostly depends upon the time domain response that the system delivers *e.g.* the rise time, percent overshoot, settling time of the output and the steady state error that exists in the final output. Also, the deflection that takes place in the arm due to its flexible nature has to be controlled because these induced vibrations reduce the performance of the system considering its accuracy and precision. This part of the literature review mainly focuses on the various modelling techniques that have been used to mathematically model a flexible arm across the world.

2.1 Review on Modelling Techniques of Flexible Link Manipulator

The most widely accepted discrete theoretical methods used to develop the dynamic model of a manipulator system having a flexible arm are listed in the following sub-sections.

2.1.1 Finite Element Method

In finite element analysis, a long structural member *e.g.* a robotic arm is divided into finite number of small elements. In case of uniform shape of object, its body is divided into number of elements having equal lengths. Each element is assumed to be connected at the end points and these end points are known as nodes. End conditions are used to study the behaviour of the elements under various conditions. The stress generated, strain developed, bending taking place in the element, displacement of each node, *etc.*,

can be found. Dynamic model of lightweight flexible arms using mathematical method like finite element method and Lagrange method was developed in the year 1986 [**Usoro *et al*., 1986**]. The link was assumed as a cascade of number of finite elements. Kinetic and potential energies were derived for each element and then were combined suitably together to obtain a final dynamic model of the entire system. A flexible arm with three degrees-of-freedom was also modelled using finite element method [**Lee** and **Wang, 1988**]. Finite Element Analysis has been used in dynamic modelling of flexible arm for tracing its trajectory [**Moulin** and **Bayo, 1990**]. The validation of this model was done using an experimental set up by comparing the simulation results and the experimental results of various outputs. Work on the feed-forward control for controlling the vibrations of the flexible arm has been done in recent years [**Mohammad** and **Tokhi, 2004**]. The theoretical model was developed based on finite element method (FEM). The validation of the research was done on the basis of system robustness, accuracy, vibration reduction and the speed of the response. FEM has been widely adopted by researchers as this method can be utilized for irregular shapes, cross sections, multiple bodies *i.e*. single link, double link, triple link, *etc*. Computers have made the computation using FEM quite easy, simpler and faster over the time. Dynamic models using FEM has shown adequate results when used with input shapers for suppressing end point vibrations [**Vaughan *et al.*, 2008**].

2.1.2 Lumped Parameter Method

Lumped dynamic model was developed for modelling flexible arms with rotary joints [**Konno** and **Uchiyanna, 1996**]. Yoshikawa and Hosoda modelled a manipulator system for N degree-of-freedom of a flexible arm using virtual rigid links and joints [**Yoshikawa** and **Hosoda, 1996**]. They developed this model for high speed machine tool and robots with elastic joints. In lumped parameter method, an entire system is modelled in the form of spring, damper and mass system. Zhu *et al*. [**1999**] used this method in their modelling and control of a manipulator system which consisted of a flexible arm. They used this method for tracking and controlling the tip of the manipulator. Khalil and Gautier [**2000**] used lumped parameter technique to model multi-body flexible system. This method is easy to apply and also quick for analysis. The disadvantage of this method is that it does not have a strong mathematical foundation.

2.1.3 Assumed Mode Method

This method had been found to be conceptually easy for developing a dynamic model of a flexible arm and hence, has been used by a number of researchers over the time for modelling flexible manipulators along with the use of Lagrange method [**Cannon** and **Schmitz, 1984; Hastings** and **Book, 1987; Konno** and **Uchiyanna, 1996; Yoshikawa** and **Hosoda, 1996; Utkin, 1998; Zhu *et al*., 1999; Khalil** and **Gautier, 2000**]. Raksha and Goldenberg [**1985**] used assumed mode method (AMM) with Newton-Euler method for deriving the equations of motion of a flexible arm. The arm was developed assuming number of truncations. Only few researchers [**Buffinton** and **Kane, 1985; Buffinton, 1992**] have worked on flexible manipulators having prismatic joints since most of the work has been done considering revolute joints. They modelled a beam moving on bilateral supports. Morris and Madani [**1997**] modelled a single link flexible manipulator considering shear deformation effect also and extended this method for utilizing it for two link flexible manipulator along with the use of Euler-Lagrange formulation.

2.2. Review on Vibration Suppression of Flexible Link Manipulator

Problems in controlling a system can be classified in two ways: regulator problem and tracking problem. Regulator problems are also called as stabilization problem. A regulator is used in a system in order to stabilize the outputs of the system and achieve equilibrium. A number of applications use the regulator approach *e.g.* the straight path maintained during the autopilot mode in vehicles for cruising, the altitude control of airplanes *etc*. Position control of a robotic arm also comes under regulator problem. In tracking control system, the control has to make sure that the output of the system traces the pre-defined trajectory which can be time varying. This control technique is used in applications like spray paintings in which the end effecter holding the paint gun has to move in a user specified direction, navigating a missile to the desired location, welding being done with the help of a robotic arm *etc*. This literature review is based on the linear controllers that have been used in controlling a flexible robotic arm. These controllers are easy to implement and understand as they are based upon a linear system. Linear controllers namely Proportional Derivative (PD) control, pole placement control and LQR control have been studied.

PD control is the simplest form of control theory which is still extensively used to control robotic arms. PD controllers are generally used for controlling the velocity and positional error of the output. This controller has been used for controlling the link deflection and joint rotation [**De luca** and **Siciliano, 1989**]. PD controllers can be used in two forms: Collocated and non-collocated. In collocated form, the sensor and actuators are placed at the same position of the joint which is to be controlled. In non-collocated form, the sensors and the actuator are not placed at the same joint which is to be controlled. The passivity property of a collocated PD controller was used to control a flexible manipulator having a single flexible arm [**Lanari** and **Wen, 1992**]. The same work was continued by De Luca and Siciliano [**1993**] for multi-link manipulator system. But, the elastic damping was not taken into account. In PD controllers, the torque applied on a joint depends completely on the velocity and the position of the joint on which it is applied. Therefore, other joints play no role in effecting the output. Hence, diagonal gain matrices are more preferred in PD controllers. This method is a widely accepted method in cases of regulation problem. Tip position control has been done using a two stage controller for a single link robotic arm [**Geniele *et al.*, 1997**]. The first stage consisted of a pole placement technique and the later stages consist of integral action. The use of LQR technique with an adaptive compensator was done for a two link manipulator system for reducing the vibrations in the link [**Bai *et al.*, 1998**]. Later, a singularly perturbed method was developed using the pole placement method for the hub angle control and tip deflection control [**konno *et al.*, 2002**]. A sliding mode controller was developed by Wilson *et al.* [**2002**]. Green and Sasaidek [**2004**] developed a trajectory tracking control for two link manipulator using inverse dynamics of a rigid link which was later improvised for flexible links with assumed modes. A detailed survey on various control methods of a manipulator system consisting of a flexible arm is done by Benosman and Vey [**2004**]. Vibration suppression was later done using LQR with non-collocated PID control for suppression of vibration which takes place at the tip of the link. LQR has also been tested for system uncertainties and parametric nonlinearities [**Khairudin *et al.*, 2011**].

2.3. National Status

The study and modelling of a flexible link manipulator has seen a tremendous increase in India in past few years. Researchers [**Krishnamurthy, 1989**] used assumed mode method for the dynamic modelling and were one among the first to study and model a flexible arm. Researchers like Theodore and Ghosal [**1995**] did a comparison of two modelling techniques that are assumed mode method and finite element method for dynamic modelling of flexible arms. Dwivedy and Eberhard [**2006**] have provided a complete literature review on the various modelling techniques that have been utilized in the past, discussing the pros and cons of every modelling technique. They have also done a detailed literature survey on the various control methods that can be used for end point vibration suppression of a flexible link manipulator. Mohan and Saha [**2007**] have done the modelling of a flexible link manipulator using Euler-Lagrange method for equation of motion and DeNOC (decoupled natural orthogonal complement) matrices for independent equation of motion. PUMA six degree-of-freedom robot has been used for illustration and validation of this method. Singla [**Singla *et al.*, 2015; Singla *et al.*, 2016**] has done an entire Ph.D. work based on the modelling of a single link as well as two link flexible manipulator using various methods like finite element method, assumed mode method, lumped parameter method. He has also done a detailed study and evaluation of various control techniques that can be used for motion tracking and end point vibration suppression. Sponsored project on design fabrication and control of flexible manipulator has been completed by IIT Guwahati under the guidance of S. K. Dwivedy and U. S. Dixit in the year 2005. A project on dynamic analysis of flexible high speed robot arm has been completed by S. K. Saha at IIT Delhi and this was funded by DST, Govt. of India and was completed on March 2006 after duration of three years. A. Singla and T. K. Bera from Mechanical department of Thapar Institute of Engineering and Technology are currently doing a DST project on development of a three link rigid-flexible manipulator for high speed operation.

2.4. Review on Application of Flexible Link Manipulators

The use of flexible arms started in space applications where robotic arms need to be light in weight as well as should be of high performance in terms of positional accuracy, speed, reduced vibrations *etc*. [**Book, 1979**]. The conventional arms which are used in

industries for production lines are required to have accurate positioning with negligible vibration. For obtaining this, the robotic arm is made of high stiffness materials. High stiffness requires heavy materials. Following problems are caused due to the use of heavy materials: they are heavy in weight, consume more power from the source for their functioning, require bigger size of actuators, heavy nature causes hindrance in transportation *etc*. Therefore, these robotic arms fall back in sectors where high speed, low support energy and accuracy are required [**Zhu *et al.,* 1999**]. Automation have increased on a very large scale in many sectors like medical surgeries, maintenance of nuclear plants, space robotics *etc*. [**Khairudin *et al.,* 2011**]. Labours have been replaced with robotic arms for various operations. Though this has reduced the labour intake but has increased the rate and accuracy of production.

2.5 Review on Bond Graph Modelling

Bond graph is a structural representation of a system in graphical form. Different energy domains of a system can be represented in a graphical form without affecting the topology of the system. This part of the literature review is based upon the application of bond graph in development of robotic arms both rigid and flexible in nature. Few other application of bond graph technique has also been listed to show its versatility in modelling. Bond graph modelling of systems belonging to different energy domains like thermal, chemical, mechanical, mechatronics, electrical *etc.* have been listed in the following sub-sections.

2.5.1 Bond Graph Modelling in Flexible Link Manipulator

The use of bond graph for mechatronic system started in the year 1991 [**Gawthrop, 1991**]. A bond graph modelling for two link rigid manipulator with flexible drives have been done. An observer control for positional accuracy of the link has been developed using bond graph [**Roberts *et al.,* 1995**]. The tachometer readings are generally contaminated with noise. Therefore, a non-linear observer was developed to estimate the velocities of the link. A closed loop system of a flexible manipulator was developed by Damic and Cohodar. A three link model was developed which had its first link rigid in nature and the other two links where flexible. This model was controlled using the controller module of the software BondSim [**Damic and Cohodar, 2006**]. A trajectory

control of manipulator system with flexible arms using the Rayleigh beam theory was later developed by Kiran *et al* [**2008**]. Bond graph modelling technique was used and the simulations were done in SYMBOLS SHAKTI software. Flexible arms which are used under water undergo various forces like hydrodynamic forces, hydrostatic forces and buoyancy forces. A Rayleigh beam model was developed for underwater flexible robotic arms [**Kumar *et al.*, 2015**].

2.5.2 Bond Graph Modelling in Various Applications

The use of bond graph for modelling complex system is done since few decades. Complex system like vehicle model has been developed by Pacejka [**1985**]. Bond graph models developed on the basis of chemical kinetics were used for electromechanical systems. Thermal models with energy dissipation were used [**Karnoop, 1990**]. Structural analysis of a system with development of control law using symbolic representation of bond graph was done [**Tanguy *et al.*, 1999**]. Dynamic loading on prismatic joints cannot be neglected as this can lead to failure of the joint. Frictional force, reaction forces at the joint and contact force of a planar slider component were found by developing a bond graph model [**Bera *et al.*, 2012**].

2.6. Observations from Literature Review

It is observed from the literature review that flexible arms tend to have low stiffness values. This in turn causes hindrance to control it when it will be in motion causing positional inaccuracy, lower repeatability and unwanted vibrations. A flexible arm imparts rigid as well as flexible nature during its working. Hence, both the nature has to be controlled which makes controlling of a flexible arm quite complex. Various methods have been adopted in modelling as well as control of such flexible arms. In order to control these arms an optimum mathematical solution should be obtained. In past few decades various mathematical modelling of flexible manipulator has been done using various methods. There are two ways of mathematically modelling a flexible manipulator they are: distributed form and discrete form. Distributed form considers the arm to have continuous distribution of parameters of the system *i.e.* mass, elasticity, damping and assumes that every part of the arm can undergo vibrations which causes infinite degrees-of-freedom of the system resulting in formation of partial differential

equations. Solutions to partial differential equations are quite difficult to achieve, whereas, discrete form is based on the assumption that the system parameters are concentrated at certain points in the system, this reduces the nonlinearity to a great extent generating ordinary differential equations which can be solved using the set of boundary conditions provided. Developing a controller based on partial differential equations formed out of distributed method is more difficult compared to development of a controller with the help of discrete method. Due to the complexity of distributed form method many researchers have used the approximated discrete method for modelling. Another point to add to the complexity is its modelling and control in applications where a certain load is present at the free end. This end point acts as a payoff load. If a payoff load is added to the free end of the flexible arm, the natural frequency of the arm changes. Hence, the vibrations induced in it during its working and stoppage changes compared to what was calculated when no pay off load was attached to the free end. Difficulty arises when the value of pay off load changes *e.g.* when different weights has to be displaced from one place to another. As the payoff load changes the natural frequency of the flexible arm changes causing difference in vibration compared to the previous value of load. Due to such reasons and fluctuation problems it makes it more difficult to be controlled hence various linear and non linear controllers are used. Linear controllers like proportional controller, PID controller, pole placement, LQR, *etc*. have been used. Using a particular controller won't solve the problem. A detailed study about the working and end point deflection values has to be studied using these controllers. In some cases, a combination of controllers has to be used for effectively controlling the flexible arm.

2.7. Objectives of Present Work

- A suitable dynamic model of a manipulator system consisting of a single flexible link would be developed using Rayleigh beam theory. This dynamic model would be developed using the structured graphical notation called bond graph.
- Validation of the dynamic model developed using bond graph would be validated with an experimental setup of flexible manipulator. The comparison would be done on the basis of the time domain response of the system and the output results obtained for the angular rotation of the hub and angle of deflection of the tip of the link.
- A control theory would be applied on the dynamic model developed using bond graph technique. The control theory would be applied to assure the rotational accuracy of the hub on which the flexible link would be mounted and reduction in the end point vibrations that are induced in link when it was rotated.

Chapter 3 Modelling of Flexible Link Manipulator

Due to the numerous limitations and disadvantages of conventional robotic arms, as discussed in previous chapter, constant research is being done in reducing the cross sectional size and weight of these robotic arms without altering their workspace. But, this in turn has caused reduction in overall stiffness of the link which makes it flexible in nature. Due to this, unwanted vibrations in the link are induced which causes reduction in accuracy and working efficiency. These draw backs can be overcome by using suitable control techniques. Therefore, a mathematical model is required for the implication of optimum control theory. In this chapter, two methods namely lumped parameter model and Rayleigh beam model have been used to model a manipulator arm which is flexible in nature and acts like a flexible link. The physical dimensions of the link and the dynamics of the actuator are kept constant in both the models. Same state variables are measured as outputs in both the theoretical models. A detailed comparison about the measured output variables as well as the performance parameters *e.g.* steady state error of the output, rise time, settling time of the output *etc.*, have been stated at the end of this chapter.

3.1 Lumped Parameter Model of a Flexible Manipulator

There are various methods to develop a theoretical model of a manipulator arm which is flexible in its nature. The finite element method, assumed mode method and lumped parameter method are the most commonly used methods. These methods are used to develop the equation of motions of the manipulator arm in order to understand the dynamics of the system.

Any set of specified variables of the system that helps in understanding and determining its response to an applied input are called as the states of the system. These states are represented in the form of matrices and this is known as state space representation. These matrices are formed with the help of the equations of motion derived from the theoretical model of the flexible arm system and they help in understanding the behaviour of the system for any applied input. MATLAB has been used for simulation. The results obtained from the theoretical model are compared with

those of the experimental values. The detailed model of a single link flexible manipulator using lumped parameter method is discussed in the subsequent sections.

3.1.1 Modelling of a Single Link Flexible Manipulator

The top view of a flexible manipulator $\overline{\text{OA}}$ rotated by an angle θ by applying a torque τ at the hub of the link is represented in Fig. 3.1. Due to the flexible nature of the link, the end point A *i.e.* the free end of the flexible link gets deflected from the reference position by a certain angle and is shown by the angle α. X and Y are the reference axis and the angles are measured from the *Y*-axis. The direction of the torque applied in the counter clockwise direction is considered as positive.

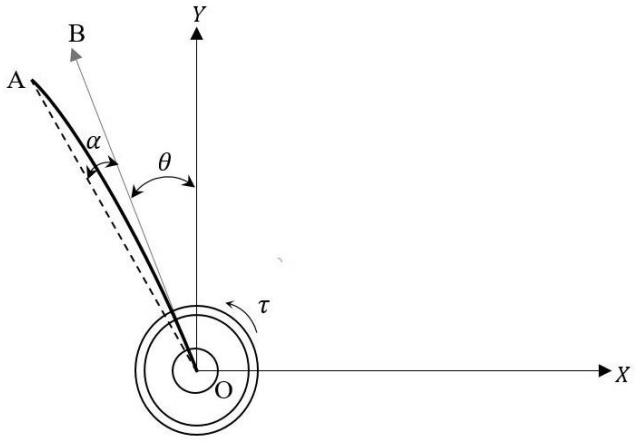

Fig. 3.1 Sketch of a rotary flexible link

The lumped parameter representation of flexible manipulator is represented in Fig. 3.2. Voltage V_{m} is given as an input to the servo motor. This voltage generates a torque τ which is applied to the hub of the flexible link with the help of gears. This torque rotates the flexible link by an angle of θ before being stopped. R_{eqv} represents the viscous friction of the servo motor. This friction applies resistance to the applied torque at the load gear. The flexible link is assumed to be a spring of stiffness K_{s} and this has an internal resistance of R_{s} which is assumed to be zero. The combined mass moment of inertia of the hub is represented with the variable J_{eqv}. The mass moment of inertia of the flexible manipulator is given by J_{s}.

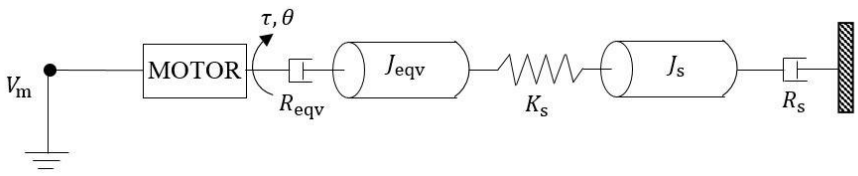

Fig. 3.2 Schema of rotary flexible link for modelling using lumped parameter method

3.1.2 System Equations

Apart from the conventional method, the Lagrange method is used in order to find the equations of motion of any system. Euler-Lagrange is a systematic approach to understand the system dynamics of a complicated system like manipulator with multiple joints. Equation (3.1) is the general Euler-Lagrange formula and it is given by

$$d/dt(\frac{dL}{d\dot{q}_i}) - \frac{dL}{dq_i} = q_i \tag{3.1}$$

The generalized co-ordinates of the system is denoted by q_i. Considering this system, let

$$q(t)^T = [\theta(t), \alpha(t)] \tag{3.2}$$

As shown in Fig. 3.1, $\theta(t)$ is the angle rotated by the servo motor and $\alpha(t)$ is the deflection taking place in the link $\overline{OA}$ due to its flexible nature. The velocities corresponding to these quantities are

$$\dot{q}(t)^T = \left[\frac{d\theta(t)}{dt}, \frac{d\alpha(t)}{dt}\right] \tag{3.3}$$

Now, by using the generalized co-ordinate mentioned above, the Euler-Lagrange equations are

$$\frac{d^2 L}{dt\, d\dot{\theta}} - \frac{dL}{d\theta} = q_i \tag{3.4}$$

and

$$\frac{d^2 L}{dt\, d\dot{\theta}} - \frac{dL}{d\theta} = q_i \tag{3.5}$$

The difference between the total kinetic energy K_{Total} of the system and the total potential energy P_{Total} in the system gives the Lagrange of any system. It can be written as

$$L = K_{\text{Total}} - P_{\text{Total}} \tag{3.6}$$

The non-conservative force like friction acts on the system with respect to the generalized co-ordinates and is given by q_i. Considering this system, the generalized forces which acts on the flexible link during its rotation are

$$q_1 = \tau - R_{\mathrm{eqv}}\dot{\theta} \tag{3.7}$$

and

$$q_2 = -R_s\dot{\alpha} \tag{3.8}$$

The servo motor applies torque at the base of the flexible link for its rotation *i.e.* at the load gear. The torque applied by the servo motor is given by

$$\tau = \frac{n_{\mathrm{g}}K_{\mathrm{g}}n_{\mathrm{m}}k_{\mathrm{t}}(V_{\mathrm{m}} - K_{\mathrm{g}}k_{\mathrm{m}}\dot{\theta})}{R_{\mathrm{m}}} \tag{3.9}$$

The complete derivation of Eq. (3.9) is given in Appendix-I. The damping of the servo motor opposes the developed torque and is given by R_{eqv}.

3.1.3 Kinetic and potential Energy

As seen in Eq. (3.6) both the mechanical forms of energies of the system needs to be determined in order to calculate the Lagrange of a given system. In this section, these mechanical energies are calculated. The translational kinetic energy is given by

$$K = \frac{1}{2}mv^2 \tag{3.10}$$

where m and v are the mass and linear velocity of the system, respectively and rotational kinetic energy can be given by

$$K = \frac{1}{2}J\omega^2 \tag{3.11}$$

where mass moment of inertia is represented by J and angular velocity is represented by ω. By using Eq. (3.10) and Eq. (3.11), it can be written as

$$K_{\mathrm{Total}} = \frac{1}{2}J_{\mathrm{eqv}}\dot{\theta}^2 + \frac{1}{2}J_{\mathrm{s}}(\dot{\theta} + \dot{\alpha})^2 \tag{3.12}$$

The potential energy of any system exists in different forms. In a mechanical system, elastic potential energy and gravitational potential energy are generally considered. The gravitational potential energy of a system can be given by

$$P_{\mathrm{g}} = mg\Delta h \tag{3.13}$$

where g is the gravitational constant, Δh is the change in height of the system from the datum or reference position. The elastic potential energy of the system can be given by

$$P_{\mathrm{e}} = \frac{1}{2} K_{\mathrm{s}} \Delta x^2 \tag{3.14}$$

In this equation, K_{s} is the stiffness of the flexible link and Δx is the linear displacement. If the flexible link flexes by a certain angle during its rotation, it stores energy. The angle of this deflection is given by α. Hence, the energy stored in the flexible link can be given as

$$P_{\mathrm{e}} = \frac{1}{2} K_{\mathrm{s}} \alpha^2 \tag{3.15}$$

It can be noted that the height of the system remains unchanged, therefore, Eq. (3.15) is the P_{Total} of the system. Now, using Eq. (3.12) and Eq. (3.15), Eq. (3.6) can be written as

$$L = \frac{1}{2} J_{\mathrm{eqv}} \dot{\theta}^2 + \frac{1}{2} J_{\mathrm{s}} (\dot{\theta} + \dot{\alpha})^2 - \frac{1}{2} K_{\mathrm{s}} \alpha^2 \tag{3.16}$$

The required derivatives are

$$\frac{dL}{d\dot{\theta}} = J_{\mathrm{eqv}} \dot{\theta} + J_{\mathrm{s}} (\dot{\theta} + \dot{\alpha}) \tag{3.17}$$

$$\frac{dL}{dt\, d\dot{\theta}} = J_{\mathrm{eqv}} \ddot{\theta} + J_{\mathrm{s}} (\ddot{\theta} + \dot{\alpha}) \tag{3.18}$$

$$\frac{dL}{d\theta} = 0 \tag{3.19}$$

After substitution of values, first equation of motion is given as

$$(J_{\mathrm{eqv}} + J_{\mathrm{s}}) \ddot{\theta} + J_{\mathrm{s}} \ddot{\alpha} + R_{\mathrm{eqv}} \dot{\theta} = \tau \tag{3.20}$$

and

$$\frac{dL}{d\dot{\alpha}} = J_{\mathrm{eqv}} \dot{\theta} + J_{\mathrm{s}} (\dot{\theta} + \dot{\alpha}) \tag{3.21}$$

$$\frac{dL}{dt\, d\dot{\alpha}} = J_{\mathrm{eqv}} \ddot{\theta} + J_{\mathrm{s}} (\ddot{\alpha} + \dot{\theta}) \tag{3.22}$$

$$\frac{dL}{d\alpha} = K_{\mathrm{s}} \alpha \tag{3.23}$$

The second equation of motion can be given as

$$J_{\mathrm{s}} \ddot{\theta} + J_{\mathrm{s}} \ddot{\alpha} + R_{\mathrm{s}} \dot{\theta} + K_{\mathrm{s}} \alpha = 0 \tag{3.24}$$

Now, by rearranging the equations, it is obtained as

$$\ddot{\theta} = \frac{R_{\mathrm{eqv}}}{J_{\mathrm{eqv}}} \dot{\theta} + \frac{K_{\mathrm{s}}}{J_{\mathrm{eqv}}} \alpha + \frac{1}{J_{\mathrm{eqv}}} \tau \tag{3.25}$$

$$\ddot{\alpha} = \frac{R_{\mathrm{eqv}}}{J_{\mathrm{eqv}}} \dot{\theta} - \frac{K_{\mathrm{s}} (J_{\mathrm{s}} + J_{\mathrm{eqv}})}{J_{\mathrm{s}} J_{\mathrm{eqv}}} \alpha - \frac{1}{J_{\mathrm{eqv}}} \tau \tag{3.26}$$

The mass moment of inertia of the link $\overline{\mathrm{OA}}$ pivoted at one end is given by

$$J_s = \frac{mL^2}{3} \tag{3.27}$$

The stiffness of the link $\overline{OA}$ is given by

$$K_s = J_s\omega^2 \tag{3.28}$$

3.1.4 Linear State-Space Model

The state-space representation is a form of representations of the state variables of the system in matrix form. These state-space equations are decoupled and each decoupled state equation will act as a sub-system. This helps in knowing whether and how each sub-system can be controlled. In this section, state-space equations and state-space representation of the manipulator arm modelled using the lumped parameter method are explained. The linear state-space equation is given by

$$\dot{x} = \mathbf{A}x + \mathbf{B}u \tag{3.29}$$

$$y = \mathbf{C}x + \mathbf{D}u \tag{3.30}$$

where *x* represents the state variable and *u* represents the control input. **A**, **B**, **C**, **D** are matrices and are known as the state-space matrices. The state variables and the output variables are

$$x^T = [\theta\ \alpha\ \dot{\theta}\ \dot{\alpha}] \tag{3.31}$$

$$y^T = [x_1\ x_2] \tag{3.32}$$

At the output, only two state variables are to be measured which are namely, the angle turned by the servo motor θ (*i.e.*, Hub angle) and the angle of deflection α. Hence, the output matrices **C** and **D** are given as

$$\mathbf{C} = \begin{bmatrix} 1 & 0 & 0 & 0 \\ 0 & 1 & 0 & 0 \end{bmatrix} \tag{3.33}$$

$$\mathbf{D} = \begin{bmatrix} 0 \\ 0 \end{bmatrix} \tag{3.34}$$

Now, by substituting x in Eq. (3.25) and Eq. (3.26), **A** and **B** matrices can be found. Substituting $\dot{x_1} = x_3$ and $\dot{x_2} = x_4$ in Eq. (3.25) and Eq. (3.26), the equations obtained are

$$\dot{x_3} = \frac{R_{\text{eqv}}}{J_{\text{eqv}}}\dot{\theta} + \frac{K_{\text{s}}}{J_{\text{eqv}}}\alpha + \frac{1}{J_{\text{eqv}}}\tau \tag{3.35}$$

$$\dot{x_4} = \frac{R_{\text{eqv}}}{J_{\text{eqv}}}\dot{\theta} - \frac{K_{\text{s}}(J_s+J_{\text{eqv}})}{J_s J_{\text{eqv}}}\alpha - \frac{1}{J_{\text{eqv}}}\tau \tag{3.36}$$

Now, matrices **A** and **B** in $\dot{x} = \mathbf{A}x + \mathbf{B}u$ can be written as

$$\mathbf{A} = \begin{bmatrix} 0 & 0 & 1 & 0 \\ 0 & 0 & 0 & 1 \\ 0 & K_{\text{s}}/J_{\text{eqv}} & -R_{\text{eqv}}/J_{\text{eqv}} & 0 \\ 0 & -K_{\text{s}}(J_{\text{s}}+J_{\text{eqv}})/J_s J_{\text{eqv}} & B_{\text{eqv}}/J_{\text{eqv}} & 0 \end{bmatrix} \tag{3.37}$$

$$\mathbf{B} = \begin{bmatrix} 0 \\ 0 \\ 1/J_{\text{eqv}} \\ -1/J_{\text{eqv}} \end{bmatrix} \tag{3.38}$$

3.1.5 Simulation Results

The matrices **A**, **B**, **C**, **D** found in Eqs. (3.33–3.38) are used in the simulation model of the flexible link manipulator to understand its behaviour for particular inputs. The MATLAB program developed for the simulation is given in Appendix-I. The actuator dynamics is also included in the state-space model which has been discussed in Eq. (3.9). The parameter values used to model rotary flexible link is given in Table 3.1. In order to simulate this dynamic system, Simulink has been used. Simulink can be used to make the graphical representation of any dynamic system to simulate and analyse it. With the help of Simulink, a step input is applied to the manipulator arm model. It is desired that the servo motor should turn at an angle of 80° for the applied step input. This model of the of the manipulator arm system is shown in Fig. 3.3. In the model, the step input block is placed at the first place. This block is available in the source block section of the Simulink library. It acts as a source of input to the system. Parameters of

the step input such as step time, initial value and final value can also be defined with the help of this block. The next block connected is the transport delay block. It is used to delay the input by a certain specified time period *i.e.* the amount of time during the simulation when the input signal is delayed from being propagated to the output. It is helpful in cases where the real system has elements which does not give an output as soon as the input is applied *e.g.* pumps, motors *etc.* The next block used is the state space block also available in the Simulink library. The state space equations developed after adding the motor dynamics given in Appendix-I are stored into this block. The values of each state space are obtained automatically from the workspace of the MATLAB program used. Initial conditions are assumed to be zero in this case. The output variables those are to be measured are the servo motor angle and the angle of deflection of the manipulator link. The next block is used to convert these outputs from radians to degree. A DEMUX block is used to split the output of the state space block into two different vectors. The scopes are used to display the outputs that have been measured. These outputs obtained are in graphical form. The entire simulation is done for a time period of 5 s. The outputs measured during the simulation are shown in Fig. 3.4. Figure 3.4 (a) shows the hub angle of rotation *i.e.* angle turned by the servo motor for the applied step input. It can be noted from the figure that the manipulator link modelled using lumped parameter method has turned more than 80° which was set as the desired angle. The steady state error of the output, rise time, settling time of the output *etc.* can be obtained and are given in Table 3.2. In Fig. 3.4(b), the angle of deflection of the manipulator link is shown. During the rotational motion of the link, deflection is observed in the entire flexible link. This figure shows the deflection of the free end of the link. Also the nature, amplitude and time period of the vibration those are induced in the link at the end of the rotational motion due to its flexible nature can be observed. The results also show that the maximum deflection lies between 6.10° and -6.11° and the deflection reaches steady state approximately at 2.5 s during simulation time period.

Table 3.1 Parameters for modelling of rotary flexible link

Parameters	Nomenclatures	Numeric values	Units
Total length of flexible link	L	0.42	m
Mass of flexible link	m	0.065	kg
Natural frequency	ω	18.5	rad/s
Flexible link stiffness	K_{s}	1.30	m/rad
Viscous friction coefficient	R_{eqv}	0.015	m/(rad/s)
Mass moment inertia of	J_{eqv}	9.76×10^{-5}	kg m^2
Mass moment of inertia of flexible link	J_{s}	3.8274×10^{-3}	kg m^2
Motor armature resistance	R_{m}	2.60	**Ω**
Motor torque constant	k_{t}	0.0077	Nm
Back-emf constant	k_{m}	0.0077	V/(rad/s)
Gear ratio	K_{g}	70	
Gear box efficiency	n_{g}	0.90	
Motor efficiency	n_{m}	0.69	

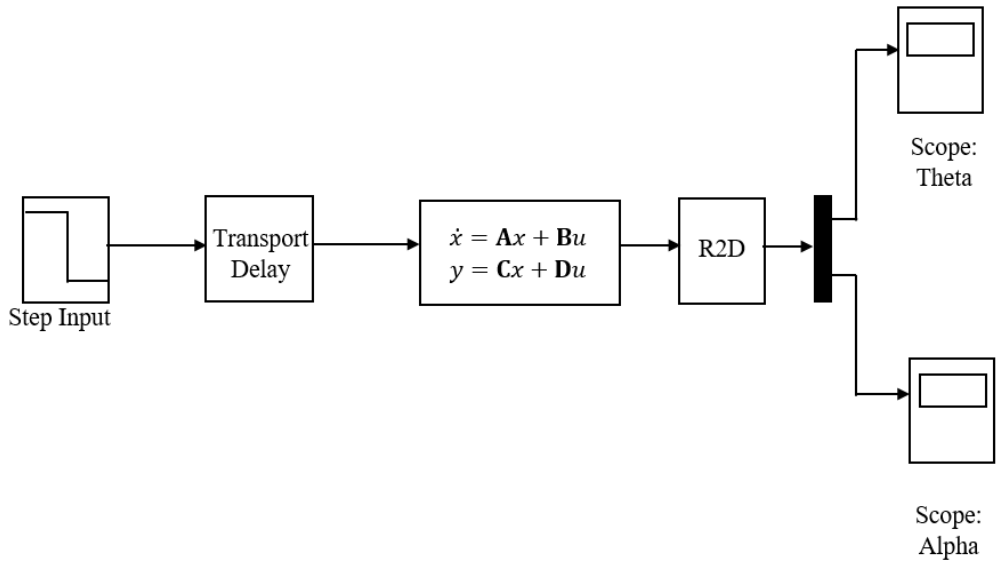

Fig. 3.3 Simulink model of rotary flexible link

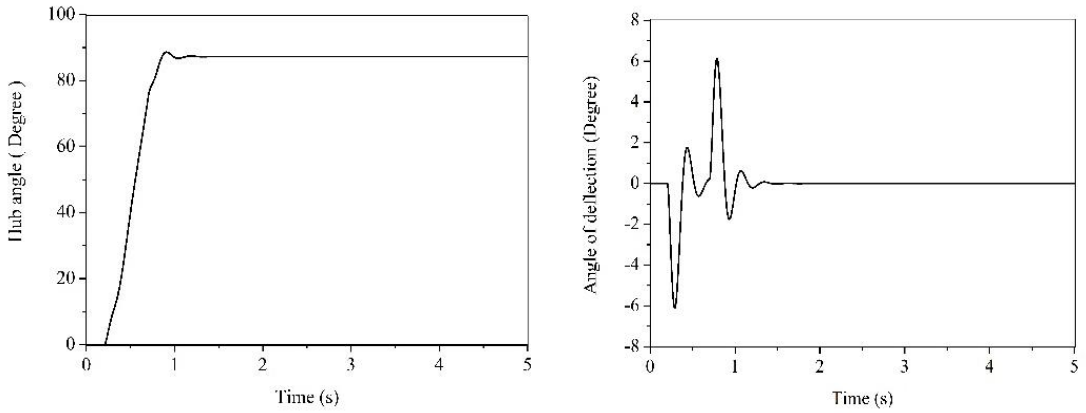

(a) (b)

Fig. 3.4 (a) Angle turned by the servo motor and (b) Angle of deflection of the free end of flexible link in lumped parameter model

Table 3.2: Performance parameters of Lumped parameter model

Model Name	Rise time (s)	Settling time (s)	Steady state error (%)	Percent overshoot (%)	Maximum deflection (°)
Lumped Parameter Model	0.76	2.73	9.03	0.98	6.10

3.2 Bond Graph Modelling of a Single Link Flexible Manipulator

In Section 3.1, manipulator arm system having a flexible link has been modelled using lumped parameter method. Servo motor angle and deflection angle of the link are considered as the main state variables. These state variables are required to be controlled in order to minimize the induced vibration during its motion. In this section, an alternative modelling method of the flexible link manipulator has been proposed. Rayleigh beam theory has been used for modelling. The comparison of the outputs obtained from the Rayleigh beam model and lumped parameter model has been made at the end of the section.

3.2.1 Rayleigh Beam Element with Generalized Forces and Displacements

In structural applications, several beam theories are being used over the years. Each of these theories has its own assumptions and limitations. The most widely used beam models in structures are namely Euler-Bernoulli beam theory, Rayleigh beam theory and Timoshenko beam theory. The Euler-Bernoulli beam theory was proposed in the year of 1750 by Leonhard Euler and Daniel Bernoulli. This theory is helpful in understanding the load carrying capacity and the deflection behaviour of a beam. The major drawback of this theory is that it assumes the beam to be under the lateral loading only. Hence, it considers only the lateral inertia while neglecting the rotary inertia. This theory has been found to work accurately for smaller beam deflection. In the year of 1894, John William Strutt, 3rd Baron Rayleigh proposed the improvement in the Euler-Bernoulli beam theory by adding the effect of rotary inertia to the beam [**Labuschagne *et al.*, 2009**]. The flexible link is assumed to be a beam having low stiffness. Therefore, a significant bending can occur in the link. Also, when a flexible beam is rotated about the fixed end by a certain angle, there is a need to consider the effect of rotary inertia during modelling. The Timoshenko beam theory was introduced in the year of 1921 by Stephen Timoshenko. This theory is an improvement to the Euler-Bernoulli beam theory. It considers the effect of shear force on the beam under the bending action [**Labuschagne *et al.*, 2009**]. However, this theory finds its applications in the areas where there is large bending of the beam and the shear force that is induced cannot be neglected. The lumped parameter method did not consider the shear force into the consideration during the modelling of rotary flexible link. Therefore, in this chapter, the Rayleigh beam theory is used to model the flexible link manipulator using the bond graph technique.

The Eulerian and Newtonian convention of forces and moments acting on an element of the beam is shown in Fig. 3.5, where F represents force and M represents moment. The relation between the generalized Newtonian forces and the generalized displacements which are acting at the end of the beam element is given by the stiffness matrix of the beam element as per Eq. (3.39). In Eq. (3.39), [K] represents the stiffness matrix of beam element.

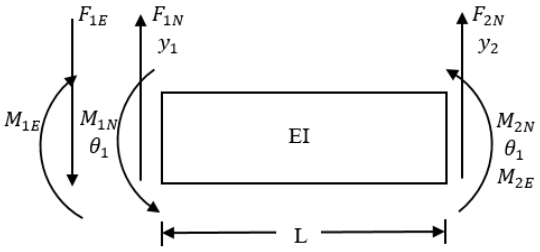

Fig. 3.5 Free body diagram of a Rayleigh beam element

3.2.2 Stiffness Matrix

The Newtonian forces and generalized displacements are related to the stiffness matrix of beam element as shown in Eq. (3.39). The stiffness matrix of Rayleigh beam element has been given in [**Mukherjee *et al.*,2006**]. In Section 3.1, Eq. (3.28) shows the stiffness K_s of the rotary flexible link and this is expressed in terms of J_s and ω. Therefore, the stiffness matrix of the Rayleigh beam element is determined in terms of mass moment of inertia J_R and natural frequency of the element ω_R. The stiffness Rayleigh beam element in form of matrix is shown in Eq. (3.40).

$$\begin{bmatrix} F_{1N} \\ M_{1N} \\ F_{2N} \\ M_{2N} \end{bmatrix} = [K] \begin{bmatrix} y_1 \\ \theta_1 \\ y_2 \\ \theta_2 \end{bmatrix} \tag{3.39}$$

$$[K] = m\omega_R{}^2 \begin{bmatrix} 1 & L/2 & -1 & L/2 \\ L/2 & L^2/3 & -L/2 & L^2/6 \\ -1 & -L/2 & 1 & -L/2 \\ L/2 & L^2/6 & -L/2 & L^2/3 \end{bmatrix} \tag{3.40}$$

Hence, putting Eq. (3.40) in Eq. (3.39) it can be expressed as

$$\begin{bmatrix} F_1 \\ M_1 \\ F_2 \\ M_2 \end{bmatrix} = m\omega_R{}^2 \begin{bmatrix} 1 & L/2 & -1 & L/2 \\ L/2 & L^2/3 & -L/2 & L^2/6 \\ -1 & -L/2 & 1 & -L/2 \\ L/2 & L^2/6 & -L/2 & L^2/3 \end{bmatrix} \times \begin{bmatrix} y_1 \\ \theta_1 \\ y_2 \\ \theta_2 \end{bmatrix} \tag{3.41}$$

3.2.3 C-Field Representation

The stiffness matrix of a beam element can be shown as a 4-port C-field element which stores energy due to the displacements that take place on the beam element [**Mukherjee *et al.*,2006**]. The manipulator system which has been modelled in Section 3.1 is not subjected to any transverse loading. Therefore, only inertial forces will be acting on the link during its rotation. Hence, in the C- field representation shown in Fig. 3.6, only rotational displacements are considered since shear force will not be taken into account during the modelling.

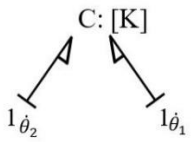

Fig. 3.6 Rayleigh beam element stiffness matrix using C-field representation

3.2.4 Space Reticulation and Inertia Lumping of Manipulator Arm

Figure 3.7 shows space reticulation and inertia lumping of a beam. The flexible link is considered as a beam with low stiffness. The flexible manipulator arm is modelled like a beam with single space reticulation at first and then it is further extended to seven space reticulations for better results.

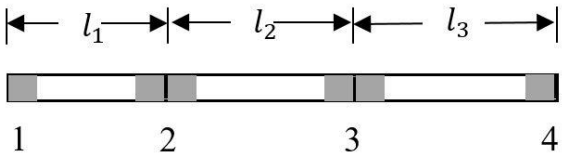

Fig. 3.7 Rayleigh beam model of flexible link with space reticulation and inertia lumping

3.2.5 Integrally Causalled Model

Rayleigh beam model for rotary flexible link is shown in Fig. 3.9. Bond graph has been used as a tool to develop this model. In this model, (RB) is the Rayleigh beam sub-program (known as capsule in bond graph lexicon) *i.e.* element which consists the

stiffness matrix of the beam and this was derived in the Eq. (3.40). This model consists of a single beam element. In Fig. 3.8, the sub-program (capsule) of Rayleigh beam is shown. This capsule considers only rotary inertia of each element in the beam. The effect of shear force is not taken into account. The flow input *i.e.* the rotational motion due to the applied torque acts as an input to the rotational port 1 of the capsule. The compliance element (C) of the capsule stores energy *i.e.* stiffness while the material damping property is denoted by R-element. The values of C and R are given in Eq. (3.42) and Eq. (3.43). The values of mass *m*, length L and the natural frequency ω are given in Table 3.1. m_{u} is the material damping coefficient of the link and is taken as 0.002. The effort output of the capsule gives the rate of change of angular displacement of the beam element. The length and mass of the element is taken equal to the length and mass of the flexible link modelled in Section 3.1. The Rayleigh beam is mounted on a hub which has mass moment of inertia J_{eq}. The Rayleigh beam model is then connected to a DC servo motor through a gear box having efficiency of n_{g} and gear ratio of K_{g}. The transformer modulus is K_{gn} which is the product of n_{g} and K_{g}. The viscous coefficient of friction is R_{eq}. The specifications of the motor like inductance and armature resistance are taken into consideration and are denoted by J_{m} and R_{m}, respectively. Both the ends of the Rayleigh beam capsule are connected to flow detectors. These flow detectors will help to measure the rate of change of angular displacement which on integration will give the angular displacements at both the ends of the Rayleigh beam element.

$$C = m\omega^2 \begin{bmatrix} \frac{L^2}{3} & \frac{L^2}{6} \\ \frac{L^2}{6} & \frac{L^2}{3} \end{bmatrix} \tag{3.42}$$

$$R = m_{\mathrm{u}} m\omega^2 \begin{bmatrix} \frac{L^2}{3} & \frac{L^2}{6} \\ \frac{L^2}{6} & \frac{L^2}{3} \end{bmatrix} \tag{3.43}$$

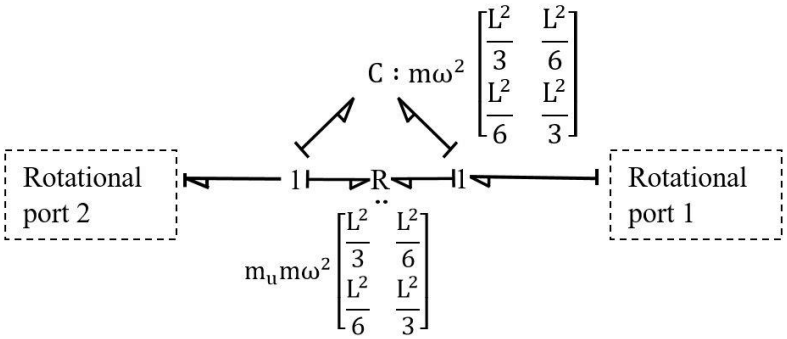

Fig. 3.8 Sub-program (Capsule) of Rayleigh beam element

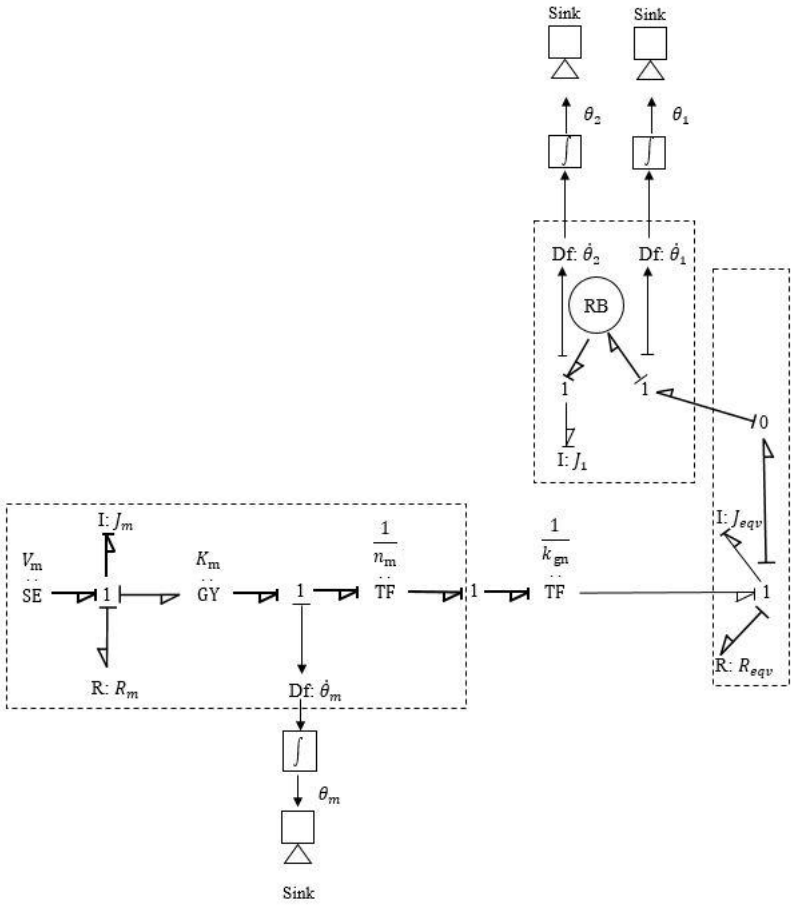

Fig. 3.9 Integrally causalled Rayleigh beam model of rotary flexible link using single Rayleigh beam element

The voltage denoted by SE element is applied to the DC servo motor. The inductance converts effort (voltage) into flow (current). The torque developed by motor depends on this current and the gyrator modulus (K_{m}) or the motor constant. The back emf depends on the angular velocity of the motor and the back emf constant. The motor

efficiency is represented by the transformer modulus (n_{m}). The transformer modulus (K_{gn}) is used to include the gear box efficiency (n_{g}) and the gear ratio (K_{g}). Further, the viscous coefficient of friction (R_{eq}) and mass moment of inertia of the hub (J_{eq}) are also taken into account. The flow detector (Df) is connected at 1-junction to measure the angular velocity of the motor.

The state variables considered to be measured are the same as taken in the lumped parameter model in Section 3.1.2. The quantities measured are namely the hub angle of rotation *i.e.* angle turned by servo motor and the angle of deflection of the free end of the flexible link. The hub angle of rotation and angle of deflection of single element Rayleigh beam model is shown in Fig. 3.10.

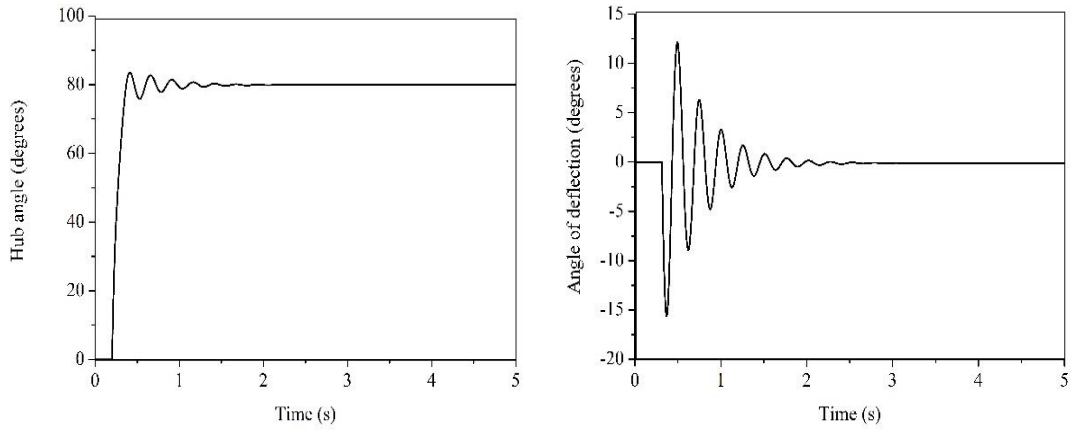

(a) (b)

Fig. 3.10 (a) Angle turned by servo motor and (b) Angle of deflection in Rayleigh beam model

The Rayleigh beam model with single Rayleigh beam element is further improvised by increasing the number of reticulations. By increasing the number of reticules for the same defined physical dimensions of the link, this model will help to achieve more detailed analysis and better measurement of the state variables needed to be measured. After modelling for a single reticule, it was decided to model the flexible link with seven number of reticules. Each of the seven element is considered of equal length and equal mass *i.e.* the flexible link is divided into seven equal parts; Fig. 3.11 shows Rayleigh beam model of rotary flexible link with seven Rayleigh beam elements. The entire working of the model is similar to that of Rayleigh beam model with single

Rayleigh beam element except that the flexible link in this case is considered as a cascade of seven Rayleigh beam capsules *i.e.* elements are connected in series. The transformer with modulus *mm* is used as a switch for transfer of motion when required.

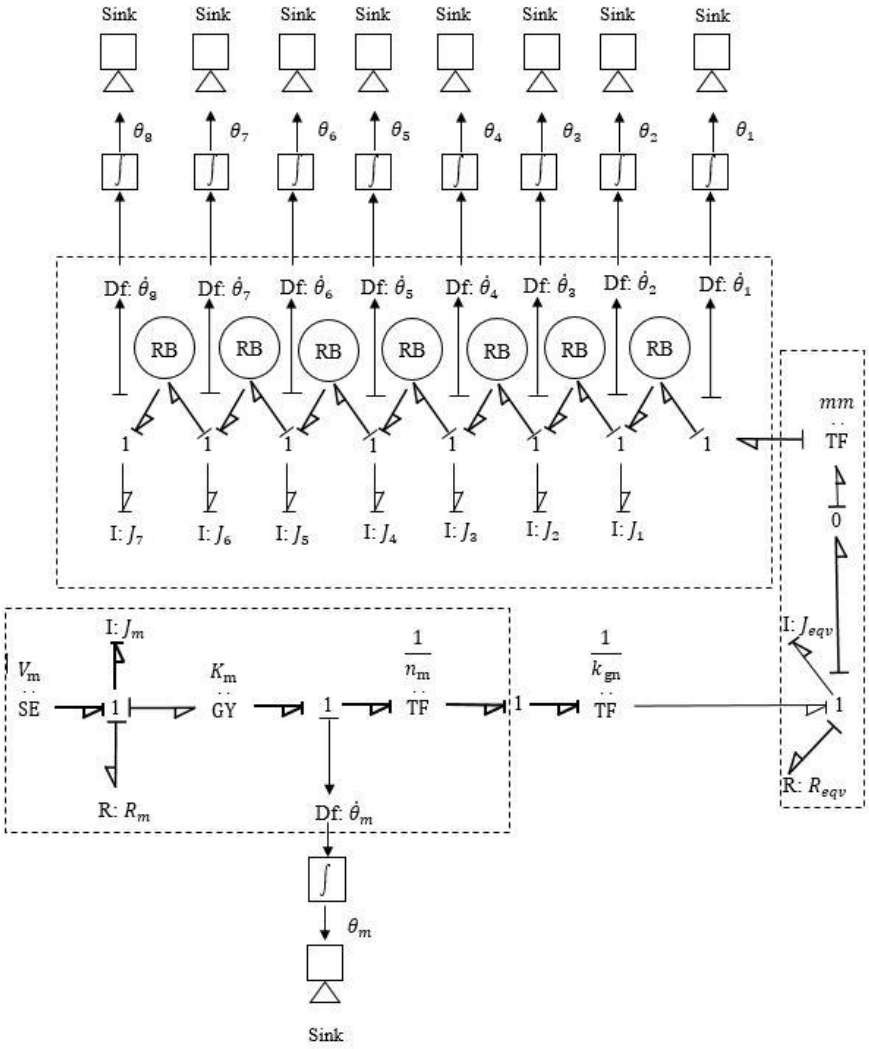

Fig. 3.11 Integrally causalled Rayleigh beam model of rotary flexible link with seven Rayleigh beam elements

3.2.6 Simulation Results

Rayleigh beam model with single Rayleigh beam element is simulated at the first place and then to achieve better results the Rayleigh beam model with seven elements is used as explained in Section 3.2.6. The simulations are done using the same numeric values for all the design parameters used for the flexible link and the actuator as given in Table 3.1. The Rayleigh beam model with seven Rayleigh beam elements recorded more link vibration compared to the Rayleigh beam model with single Rayleigh beam element. Figure 3.12 shows the hub angle of rotation and angle of deflection of the Rayleigh beam model with seven Rayleigh beam elements. The simulation time period is kept constant in the simulation for both lumped parameter model and Rayleigh beam model. The combined results of all the performance parameters are shown in the Table 3.3. This table shows the error in the desired output, the range of maximum deflection as well as other parameters required to study the system. In the Table 3.4, a comparison of both the theoretical models has been made. All the parameters measured with the help of the measured outputs in both the models are stated together along with the range of maximum deflections taking place in the link. This table helps in a comparative study of the models.

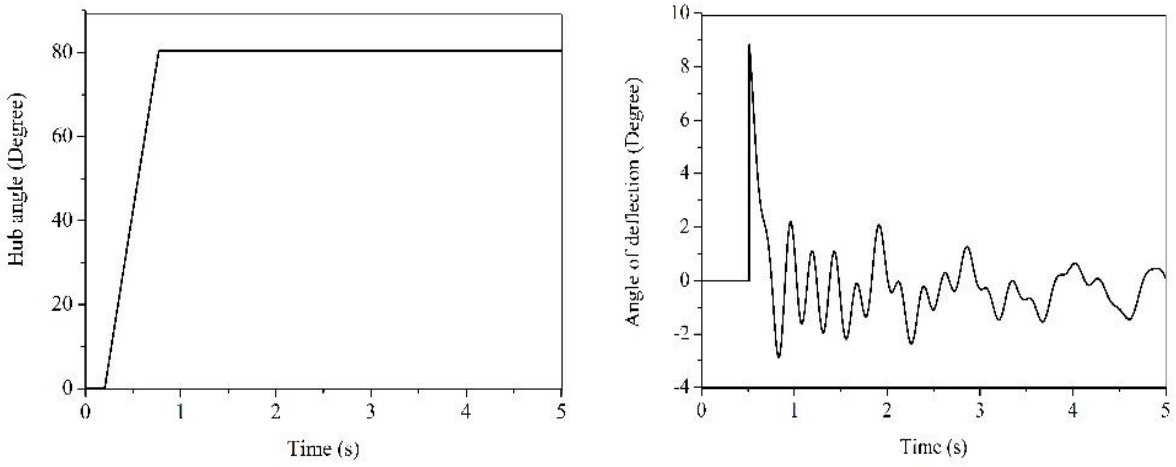

(a) (b)

Fig. 3.12 (a) Angle turned by the servo motor and (b) Angle of deflection of flexible link in Rayleigh beam model with seven elements

Table 3.3 Performance parameters of Rayleigh beam model

Method	Rise time (s)	Settling time (s)	Steady state error (%)	Percent overshoot (%)	Maximum deflection (°)
Rayleigh beam model using bond graph	0.77	0.77	0.45	0	8.83

Table 3.4 Comparison between Lumped parameter model and Rayleigh beam model

Model Name	Rise time (s)	Settling time (s)	Steady state error (%)	Percent overshoot (%)	Maximum deflection (°)
Lumped parameter model	0.76	2.73	9.03	0.98	6.10
Rayleigh beam model using bond graph	0.77	0.77	0.45	0	8.83

Chapter 4 Experimentation of Single Link Flexible Manipulator

In Chapter 3, two different methods are discussed to theoretically model a flexible manipulator. The simulation results of both the methods have been compared in Table 3.4. In order to know how accurately these dynamic models, predict the output of an actual manipulator arm, an experimental setup has been used and tested. In this chapter, an experimental setup of flexible manipulator is discussed. As discussed in Chapter 3, the two state variables that are to be known and controlled in order to achieve the desired output from a manipulator arm are the angle of rotation of the servo motor and the deflection that takes place in the link because of being flexible in nature. The flexible nature of the link is caused because of the cross section of the beam being very less in comparison to its length. The experimentation will help in comparing the results with the dynamic models of the actual system developed in Chapter 3. The functionality of the experimental setup is similar to the theoretical models made in lumped parameter method and Rayleigh beam method. The rotation of the link takes place in the horizontal plane. The dimensions of the flexible link and the actuator specifications are mentioned in Table 4.1 and Table 4.2. Two outputs that have been measured from the experimental setup are the angle of rotation of the servo motor using an optical encoder and the deflection that takes place in the link measured using a strain gauge. A potentiometer has also been attached to the manipulator system in order to measure the voltage required to rotate the link by a certain angle. The different sensors used and the experiment conducted are discussed in the subsequent sections.

4.1 Description of Setup

A flexible manipulator is shown in Fig. 4.1. The link consists of a scale made of stainless steel and this is assumed to be a flexible link since the cross sectional area of the link is very less with respect to its length. This induces bending in the scale on application of load. The link is pivoted at one end and is mounted on a DC servo motor through a hub with a gear train arrangement. The servo motor attached to the flexible link provides horizontal motion to the link. A strain gauge is positioned at the clamped end of the stainless steel link. The strain gauge detects the deflection that takes place at the free end of the link during its horizontal motion. The output received from the strain gauge is in form of analog signals and is proportional to the deflection that takes place

at the free end. The encoder which is placed below the pivoted end of the flexible link records the angle turned by the servo motor. All the elements in the system are discussed in Section 4.2.

Fig. 4.1 Experimental setup of single link flexible manipulator

4.2 Component Nomenclature

The nomenclature of every component used in the flexible link setup is given in Table 4.1. Figure 4.2 represents each part of the flexible link setup according to its nomenclature given.

Table 4.1 Elements of manipulator arm system

ID	Component	No.	Specifications	Functions
1	Base	1	-	The manipulator system is mounted on it
2	Control board	1	-	It works as a circuit board on which strain gauge circuit, potentiometer circuits and sensor connector are mounted
3	Flexible link	1	42cm×0.1cm×2cm	It acts as a flexible arm
4	Strain gauge	1	Measurement range ±5V with a calibration gain of 1/16.5 rad/V	It measures the deflection at the tip of the link
5	Sensor connectors	1		It is used to transmit data from the sensors to the data acquisition board
6	Potentiometer	1	Single turn 10 kΩ sensor with electrical range of 352°	It is used to measure the input voltage

7	Encoder	1	Optical shaft encoder with 4096 resolution	Measures the angular rotation of the servo motor
8	Tachometer	1	6 pin mini DIN	It measures the rpm of the servo motor
9	Motor	1	It is a 6V DC motor with power output of 3.23W	It is used to rotate the flexible link
10	Motion pinion	1	24 teeth	It transfers the motion from the motor shaft to the load gear
11	Load gear	1	120 teeth	It transfers the angular motion from the motion pinion to the hub
12	Potentiometer anti-backlash gear	1	-	It is mounted on the potentiometer
13	Ball bearing block	1	-	It is used for smooth rotational motion of the hub

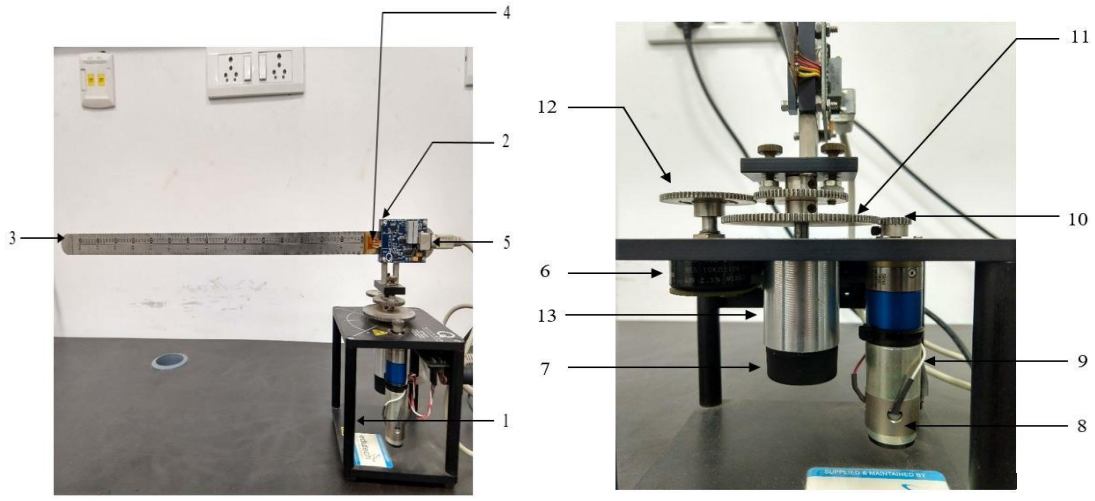

(a) (b)

Fig. 4.2 (a) Side view of flexible manipulator hardware and (b) Front view of flexible manipulator hardware

Base: The entire system of the manipulator arm is mounted on it. Elements such as servo motor, encoder, potentiometer, tachometer *etc.* are placed on it.

Control board: This circuit board consists of strain gauge circuit, offset potentiometer, gain-potentiometer and sensor connector. This element of the system plays the role in transferring the strain gauge output to the data acquisition card.

Flexible link: This is a scale made up of stainless steel with Young's modulus of 180 GPa and mass of 0.065 kg. This scale has low stiffness and therefore, it is assumed as a flexible arm.

Strain gauge: It is used to measure the vibrations of the tip of the link. It gives output in the form of analog signals proportional to the deflection taking place at the tip of the link

Sensor connector: This port is used to connect the control board to the data acquisition card. The output signals from the strain gauge and other components on the module are transferred from this port.

Potentiometer, encoder and tachometer are used to measure the voltage of the motor, angular rotation of the motor and the angular speed of the motor, respectively. A 6V motor is used to rotate the flexible link by a pre-set angle. The motor rotation is transferred to the link through the motor pinion gear and the load gear. The ball bearing block is used for the smooth rotation of the link.

4.3 Working Principle of Flexible Manipulator

The flexible manipulator hardware setup is powered by Simulink. A data acquisition card and an amplifier are connected for recording the outputs from the sensors and amplifying the signals, respectively. A servo motor of 6V is mounted on the base on which the flexible link is placed. This motor will provide horizontal motion of the link *i.e.* the link will rotate in the horizontal plane when rotated by the motor. When a step input is provided to the hardware system, the motor turns the hub (on which the link is mounted) by a certain angle. This angle depends on the amplitude of the step input applied. As the amplitude of the step input increases, the angle turned by the motor increases. The angular rotation made by the servo motor is recorded with the help of an optical encoder which has a resolution of 4096. The encoder is placed just below the bearing block as shown in Fig. 4.3. In the back end, the encoder is connected to the data acquisition card. The result recorded by the encoder is continuously sent to the data acquisition card during experimentation. A potentiometer is also connected to the load gear using an anti-backlash gear. This potentiometer records the voltage being applied.

The deflection at the tip of the link is measured with help of a strain gauge which is mounted at the pivoted end of the link as shown in Fig. 4.2. The strain gauge sends the output in form of analog signals which are proportional to the deflections being produced. These data are retained into the data acquisition card from which it becomes accessible for the Simulink model. The results of the measured outputs are displayed with the help of scope. The outputs displayed are the angle rotated by the servo motor for the applied step input and the deflection that occurs in the link due to the rotational motion of the link. The values of all the parameters required for the experimentation of the flexible link system are stated in Table 4.2.

Table 4.2 Parameters used for experimentation

Parameters	**Nomenclatures**	**Numeric values**	**Units**
Voltage	V_{m}	6	V
Motor armature resistance	R_{m}	2.60	Ω
Total length of flexible link	L	0.42	M
Mass of flexible link	m	0.065	kg
Natural frequency	ω	18.5	rad/s
Flexible link stiffness	K_{s}	1.30	m/rad
Back-emf constant	k_{m}	0.0077	V/(rad/s)
Viscous friction coefficient	R_{eqv}	0.015	m/(rad/s)
Mass moment inertia of hub	J_{eqv}	9.76×10^{-5}	kg m^2
Mass moment of inertia of flexible link	J_{s}	3.8274×10^{-3}	kg m^2
Motor torque constant	k_{t}	0.0077	N m
Gear box efficiency	n_{g}	0.90	
Motor efficiency	n_{m}	0.69	
Gear ratio	K_{g}	70	

In Fig. 4.4, the Simulink model of flexible manipulator is shown. The working of the system is as follows: a source block is used to apply an input to the hardware system. This block is available in the Simulink library under the source menu. The input applied is a step input. The amplitude and time period of the input can be set inside the block. The input is passed through a time delay block which is useful in cases where the system does not produce an output as soon as the input is applied *e.g.* pumps, motors *etc.* It is used to delay the input by a certain specified time period *i.e.* the amount of time during the simulation when the input signal is delayed from being propagated to the output. The next block represents the entire hardware of the flexible manipulator *i.e.* it includes

the motor, the gearbox, the hub, strain gauge, encoder *etc.* The output received at the data acquisition card is read and then transferred to the scope. The R2D block is used to convert the measurements taken in radians into degrees. The theta scope shows the angular rotation made by the servo motor and the alpha scope shows the deflection that takes place on the free end of the link.

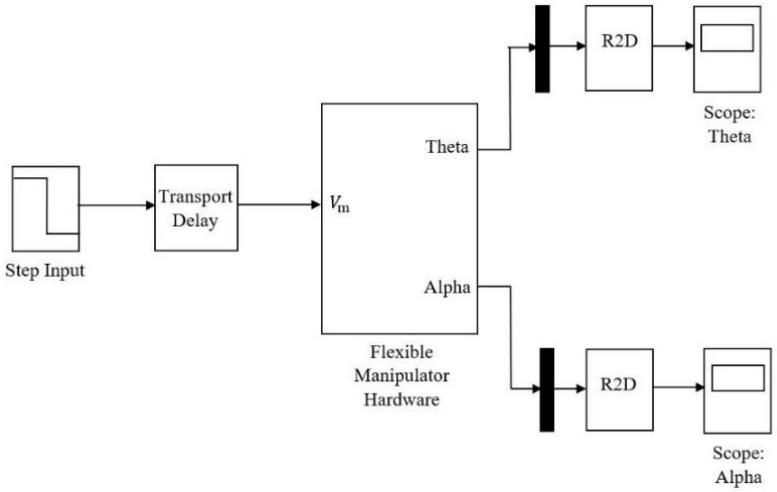

Fig. 4.3 Simulink model of flexible manipulator

4.4 Experimentation Results

The results of the angular rotation made by the motor and the deflection that takes place in the link during the rotational motion are shown in graphical forms in Fig. 4.4 (a) and (b), respectively. From Fig. 4.4 (a), it can be noted that the motor turns slightly less than the desired output of 80°. The rise time, percentage overshoot, steady state error, settling time of the output *etc.* can be obtained from the result and are shown in Table 4.3. Figure 4.4 (b) shows the vibrations that are induced into the tip of the link during its working. The maximum range of deflection, nature of vibration, settling time of vibration, *etc.* can be obtained from the result. The maximum deflection is stated in Table 4.3.

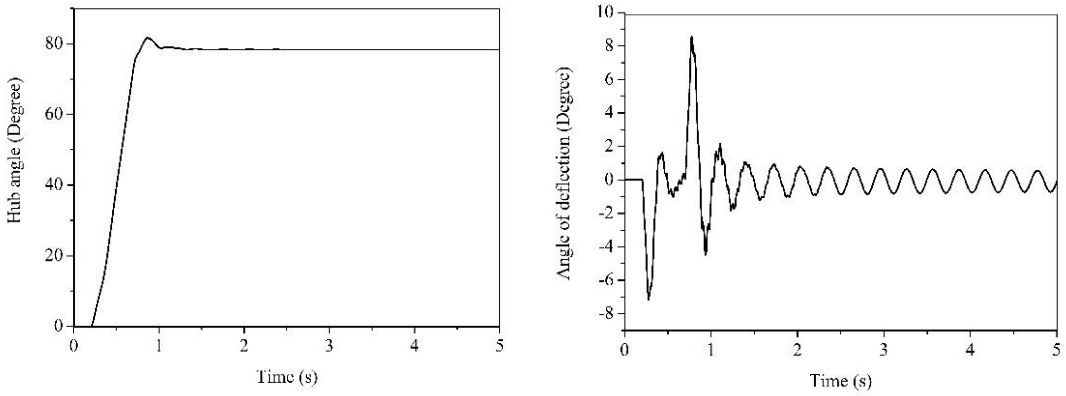

(a) (b)

Fig. 4.4 (a) Angle turned by the servo motor and (b) Angle of deflection of flexible link in experimentation

Table 4.3 Performance parameters of flexible manipulator

Method	Rise time (s)	Percent overshoot (%)	Steady state error (%)	Settling time (s)	Maximum deflection (°)
Flexible manipulator	0.81	4.27	2.11	2.40	8.58

4.5 Comparison of Results

The subsequent sections show the comparison of the outputs obtained from experimentation of the flexible manipulator with the outputs of both the dynamic models of flexible manipulator explained in Chapter 3. The comparison of the performance parameters and the maximum range of deflection of both the dynamic models along with results obtained from the experimental setup are stated together in Table 4.5.

4.5.1 Lumped Parameter Model *vs*. Experimentation

In Fig. 4.5 (a) and (b), the outputs of the dynamic model of flexible manipulator modelled using the lumped parameter method is compared with the output obtained from the actual hardware setup of the flexible manipulator. The states measured in both the cases are the angle of rotation of the motor and the deflection induced in the tip of the link. The solid black line shows the output obtained from the dynamic model of

lumped parameter model and the grey line represents the output from the actual hardware setup. In Fig. 4.5 (a) it is seen that the angle turned by the dynamic model is neither closer to the desired angle of 80° nor it is closer to the experimental value. It can be said that the lumped model overestimates the angular rotation of the hub *i.e.* servo motor. In Fig. 4.5 (b), the vibration shown by the lumped parameter model follows exactly the same pattern of vibration induced during experimentation for the first few seconds but then damps quickly. Also the maximum deflection estimated is less than the actual. Hence, it can be said that the lumped model underestimates the induced vibrations. Table 4.4 shows the comparison of the performance parameters and the maximum deflection.

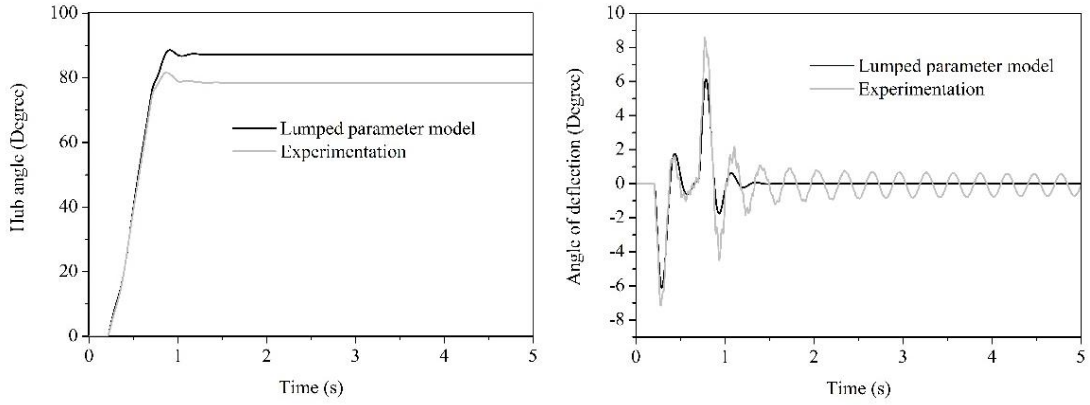

(a) (b)

Fig. 4.5 (a) Angle turned by the servo motor and (b) Angle of deflection of flexible link in Lumped parameter model and experimentation

Table 4.4 Comparison of performance parameters of lumped parameter model and experimentation

Method	**Rise time (s)**	**Percent overshoot (%)**	**Steady state error (%)**	**Settling time (s)**	**Maximum deflection (°)**
Lumped parameter model	0.76	0.98	9.03	2.73	6.10
Flexible Manipulator	0.81	4.27	2.11	2.40	8.58

It can be noted from Table 4.4 that the rise time of the theoretical model is less compared to the actual rise time recorded during the experimentation. The percentage of overshoot is obtained quite low in the theoretical model whereas the actual system has an overshoot of 4.27% which is quite higher than the predicted result. This shows

that the manipulator setup is an under damped system. The steady state error given by the theoretical model is very high compared to the error which has been obtained during the experimentation. The steady state error of 9.03% has been obtained from the theoretical model whereas only 2.11% is obtained during the experimentation. This error has to be removed in order to achieve the desired angular rotation. Also, the theoretical model predicts settling time of the output more than the settling time noted during experimentation. The maximum deflection of the link recorded from the theoretical model is less compared to the maximum deflection obtained from experimentation. It can be the excessive overshoot observed in the experimental setup because of it being an under damped system. The parameters which are to be optimised in order to get the desired output of the state variables measured are mainly the steady state error and the maximum deflection. The difference between the other parameters of performance is quite low and hence, can be given minimal importance.

4.5.2 Rayleigh beam model *vs*. Experimentation

In Fig 4.6 (a) and (b), the outputs measured from the dynamic model of flexible manipulator made using the Rayleigh beam model of seven elements is compared with the output obtained from experimentation of the flexible manipulator. The states measured in both the cases are the angle of rotation of the motor and the deflection induced in the link. The solid black line shows the output obtained from the dynamic model of Rayleigh beam model and the grey line represents the output from the actual hardware setup. In Fig. 4.6 (a), it can be seen that the angle turned by the dynamic model is closer to the desired angle of 80° compared to the angle turned by servo motor during experimentation. Rise time, percent overshoot, steady state error, settling time *etc.* are given in Table 4.5. In Fig. 4.6 (b), it can be noted that the vibrations shown by the Rayleigh beam model does not exactly match with the experimentation result but the nature of vibration, time period, maximum deflection, *etc.* are closer to the experimental results. Table 4.5 shows the comparison of the performance parameters and the maximum deflection.

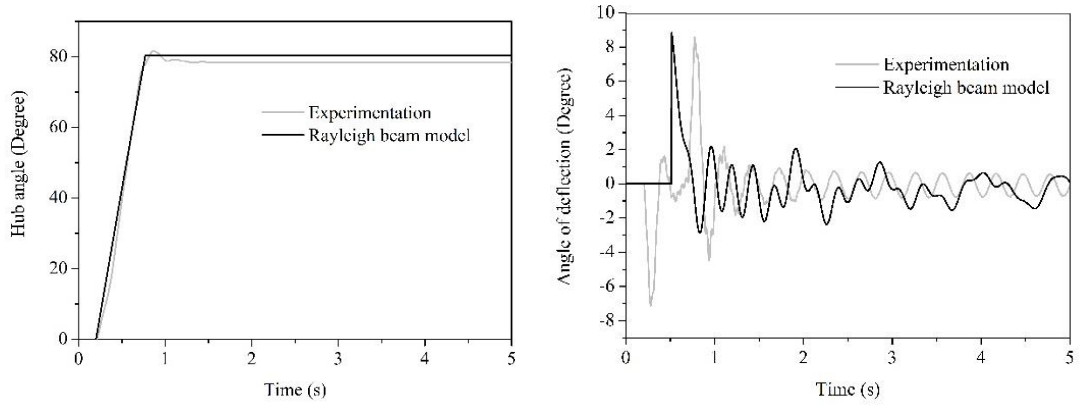

(a) (b)

Fig. 4.6 (a) Angle turned by the servo motor and (b) Angle of deflection of flexible link in Rayleigh beam model and experimentation

Table 4.5 Comparison of performance parameters of Rayleigh beam model and experimentation

Method	**Rise time (s)**	**Percent overshoot (%)**	**Steady state error (%)**	**Settling time (s)**	**Maximum deflection (°)**
Rayleigh beam model using bond graph	0.77	0	0.45	0.77	8.83
Flexible Manipulator	0.81	4.27	2.11	2.40	8.58

It can be seen in Table 4.5 that the rise time obtained from the dynamic model of the flexible manipulator is slightly less than the time required during experimentation. The dynamic model predicts zero overshoot of the flexible manipulator whereas in reality, an overshoot of 4.27% occurs. The steady state error difference between the Rayleigh beam model and the actual setup is less compared to the steady state error difference observed in lumped parameter model. The maximum deflection predicted by the Rayleigh beam model is nearer to the maximum deflection obtained during the experimentation of the flexible manipulator. Steady state error and the maximum deflection are to be controlled in order to obtain desired angular rotation and minimum or no vibration in the manipulator link.

4.5.3 Comparison between Bond Graph Model, Lumped Parameter Model and Experimentation

In Fig 4.7 (a) and (b), the outputs measured from the dynamic models of flexible manipulator using the lumped parameter model and the Rayleigh beam model of seven elements are compared with the output obtained from the actual hardware setup of the flexible manipulator. The states measured in all the cases are the angle of rotation of the motor and the deflection induced in the link. The solid black line shows the output obtained from the dynamic model made of Rayleigh beam model; the black dashed line represents the output obtained from the lumped parameter method and the grey line represents the output from the actual hardware setup. In Fig. 4.7 (a), it can be noted that the Rayleigh beam model is closer to 80° compared to the rest two outputs. The percentage overshoot is zero and the steady state error is the least in the Rayleigh beam model. The settling time obtained is also the least in the Rayleigh beam model while the lumped parameter method over predicts the settling time. In Fig. 4.7 (b), it can be noted that the vibrations shown by the Rayleigh beam model does not exactly match with the experimentation result but the nature of vibration, time period, maximum deflection *etc.* are closer to experimentation. The vibration shown by the lumped parameter model follows exactly the same pattern of vibration induced during experimentation for the first few seconds but then damps quickly. Also, the maximum deflection estimated is less than the actual. Hence, it can be said that the lumped model underestimates the induced vibrations. Table 4.6 shows the comparison of the performance parameters and the maximum range of deflection of all the three models.

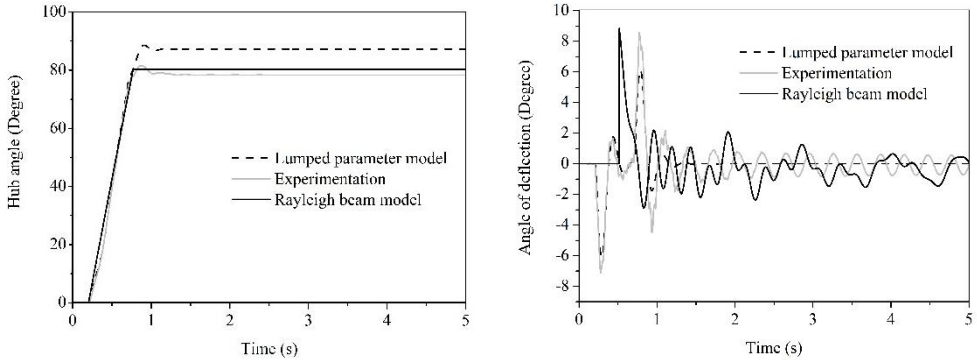

(a) (b)

Fig. 4.7 (a) Angle turned by the servo motor and (b) Angle of deflection of flexible link

Table 4.6 Comparison of performance parameters of Rayleigh beam model, lumped parameter model and experimentation

Method	Rise time (s)	Percent overshoot (%)	Steady state error (%)	Settling time (s)	Maximum deflection (°)
Rayleigh beam model using bond graph	0.77	0	0.45	0.77	8.83
Flexible Manipulator	0.81	4.27	2.11	2.40	8.58
Lumped parameter model	0.76	0.98	9.03	2.73	6.10

The steady state error predicted by the Rayleigh beam model is the least whereas it is the maximum in the lumped parameter model. The difference between the steady state error obtained from actual experimentation with both the dynamic models is the least when taken with the Rayleigh beam model, while it is the highest when taken with the lumped parameter model. The maximum deflection obtained in Rayleigh beam model is closer to the maximum deflection observed during the experimentation. These two parameters play major role in deciding whether the system is producing the desired outputs; hence, these two parameters are majorly used as the basis of comparison between the dynamic models and the experimentation.

Chapter 5 Control of Single Link Flexible Manipulator

A controller is to be used when the output generated by the system is not equal or near to the desired or pre-set output values. As discussed in earlier chapters due to the cross sectional area of the arm is very small compared to its length; the link becomes flexible in nature due to this; vibrations are induced in the link on application of load or when it is rotated by a certain angle. Also, the angle rotated by the servo motor in both the dynamic models made in Chapter 3 and during the experimentation in Chapter 4 is not exactly equal to the desired output of 80°. In order to achieve desired angular rotation and minimize the vibrations in the link, certain states of the system are to be controlled using a suitable control theory. For this purpose, various controllers are to be used. These controllers vary the performance parameters of the system in order to deliver the desired results. In this chapter, three controllers have been modelled for the Rayleigh beam model and their effects on various performance parameters of the system have been discussed. The main performance parameters modified to achieve the desired output are the state steady error of the output and the maximum deflection that takes place in the link during its rotational motion. The controller which was able to deliver the output results of the Rayleigh beam model closer to the desired output has been suggested. This controller has also been designed for the lumped parameter model and has been applied on the experimental setup. All the results obtained from the dynamic models and experimentation have been compared and stated in the subsequent chapters.

5.1 Controllability and Observability of Bond Graph Model

Controllability of the system refers that any system which can be taken from an initial state $x(t_0)$ to final state $x(t_f)$ in a finite time $(t_f - t_0)$ with the application of control input $u(t)$ where $t_0 < t < t_f$ is said to be controllable system. The state equations formed using the equations of motion help to decouple the system. Each decoupled equation will work as a sub-system. This helps to know whether each state is affected by the control input $u(t)$. If any sub-system is unaffected by the control input, the following sub-system is uncontrollable. There are many reasons which can cause an uncontrollable system and this can be studied in detail in various books. Therefore,

controllability of the dynamic model is to be checked. The controllability of system is given by

$$\mathbf{P} = \mathbf{B}\ \mathbf{AB}\ \mathbf{A^2B}\ .\ \ldots\ \ldots\ \ldots\ \mathbf{A^{n-1}B} \tag{5.1}$$

In Eq. (5.1), **P** is the controllability matrix, $\mathbf{A}_{n\times n}$ is the system state coefficient matrix of x_i state variables where i= 1, 2, 3…., n and **B** is the input matrix. A system is said to be controllable when the rank of its controllability matrix is equal to n. In order to apply a control theory for controlling certain states of the dynamic models made in Chapter 3, it is required that all the states of the system are also observable. Many times not all the states of the system are measureable using a sensor; hence, these states are to be estimated for their initial conditions using an observer. Therefore, in order to apply a control theory to dynamic models made in Chapter 3, it is necessary to check whether these models are completely observable and controllable. The controllability and observability of both the models are given in Appendix II. Both the models are found to be controllable and observable. In order to get the desired output of the system, a controller modifies the system parameters. The next step is to decide the time domain requirements so that the control theory which is going to be used has certain reference to be compared. The characteristics of controller are given in Table 5.1.

Table 5.1 Characteristics of controller

Parameter	Allowable limit
Settling time	t_s<=1s
Percentage overshoot	P_o<= 3%
Steady state error	e_{ss}<=3%
Maximum deflection	α_m<=10°
Control input	V_m<= 10V

The controller being used must satisfy these mentioned conditions. All these parameters must not exceed their allowable limit. Along with the outputs, the control theories will be compared on their time domain performance also.

5.2 Full State Feedback Control of Rayleigh Beam Model using Bond Graph

The transfer function obtained from a dynamic system represents the differential equation of the system, while the system response is decided by the poles and the zeros of the system. In any dynamic system, the poles of the system decide whether the system is controllable or not. The response of an unforced SISO system with some initial condition is given by the expression

$$y(t) = \sum_{i=1}^{n} C_i e^{\lambda_i t} \tag{5.2}$$

where n is the order of the system, C_i are the constants and λ_i are the roots of the system. These roots of the system are called the eigenvalues. If these eigenvalues are positive, Eq. (5.2) will show a never ending increase in its value. This shows that for a certain input, the system will have a never ending response. If these eigenvalues are negative, Eq. (5.2) shows values in reducing order. This leads to the conclusion that positive eigenvalues cause an unstable system while negative values of the eigenvalues make the system stable in nature *i.e.* it can be controlled to get a desired output. In the classical methods of controlling a system, the transfer function of the system is varied till the desired performances are obtained from the closed loop system. The performance of these closed loop systems is indicated by the frequency response of the system or the poles of the system. For larger order systems, it becomes difficult to vary the transfer function in a specific manner and only few poles of the closed loop system can be altered but not all the poles can be relocated. Also in classical approach, sometimes it is not possible to control every pole independently *i.e.* the change in location of one pole alters the location of certain other poles of the system also. Hence, the desired output may not be possible to achieve. This makes their applications limited to lower order systems and SISO systems. Therefore, modern control theory is used to control the system.

In a full state feedback controller, all the state variables of the system are measured. These state variables are then multiplied by some gain value (k) in order to modify their response and to achieve the desired output. The full state feedback controller is also known as pole placement method because in this control theory, the poles of the system are relocated to the positions where the system is able to generate

the exact required output. The general layout of pole placement controller is shown in Fig. 5.1.

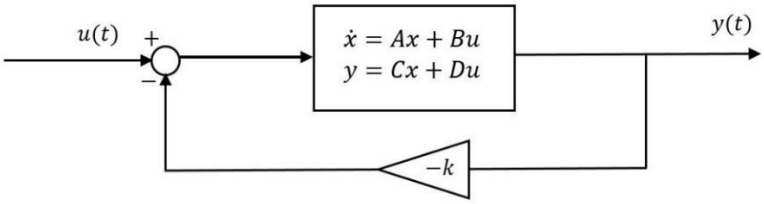

Fig. 5.1 Schema diagram of full state feedback controller

In Fig. 5.1, $u(t)$ is the control input given to the system represented by

$$\dot{x} = \mathbf{A}x + \mathbf{B}u \tag{5.3}$$

$$y = \mathbf{C}x + \mathbf{D}u \tag{5.4}$$

where **A** is the state coefficient matrix and **B** is the input matrix. **C** and **D** are the output matrix of the system; x represents the states of the system. The states of this system are measured using suitable sensors and their outputs are taken as feedback. This feedback of each state is multiplied by a gain value of k and is then again sent back as an input to the system. This is how every desired state is controlled and required output is obtained from the system. The control input of a system is given by the equation

$$u = -\mathbf{k}x \tag{5.5}$$

If the value of the control input is replaced in Eq. (5.3), the modified equation becomes

$$\dot{x} = \mathbf{A}x + \mathbf{B}(-\mathbf{k}x) \tag{5.6}$$

$$\dot{x} = (\mathbf{A} - \mathbf{B}\mathbf{k})x \tag{5.7}$$

where $(\mathbf{A} - \mathbf{B}\mathbf{k})$ gives the closed loop state coefficient matrix $\mathbf{A}_{cl}$. The poles also called as the loop poles of this particular system are the eigenvalues obtained from $\mathbf{A}_{cl}$ *i.e.* state coefficient matrix. Therefore, by appropriate selection of the eigenvalues, the poles of the

system can be relocated and the states can be controlled which in turn will help in generating desired output from the system. Now, a plant having an order n and number of input r, the gain matrix **k** is of the size $r \times n$. As the numbers of inputs increase the design parameters available also increase and it becomes easy to select the location of the poles. The state coefficient matrix **A**, input matrix **B** and the output matrices **C** and **D** of the Rayleigh beam model of single link flexible manipulator arm are given in Appendix III. The last state represents the rotation of the hub (θ_1) and the second last state represents the displacement of the tip of link (θ_2) among five state variables. First three state variables correspond to the momentum of the system. The gains that can lead to the desired output of the system are calculated by using

$$|\lambda \mathbf{I} - \mathbf{A}_{cl}| = 0 \tag{5.8}$$

where after substitution of appropriate eigenvalues λ, the gain matrix **k** is generated. In Appendix III, the state coefficient matrix $\mathbf{A}_{cl}$ is calculated and the suitable gains for the system are calculated by setting the poles *i.e.* the eigenvalues of the system at desired location. These gain values are multiplied by the corresponding states of the system and are sent as an input to the system. The full state feedback control of the Rayleigh beam model using bond graph is shown in Fig. 5.2.

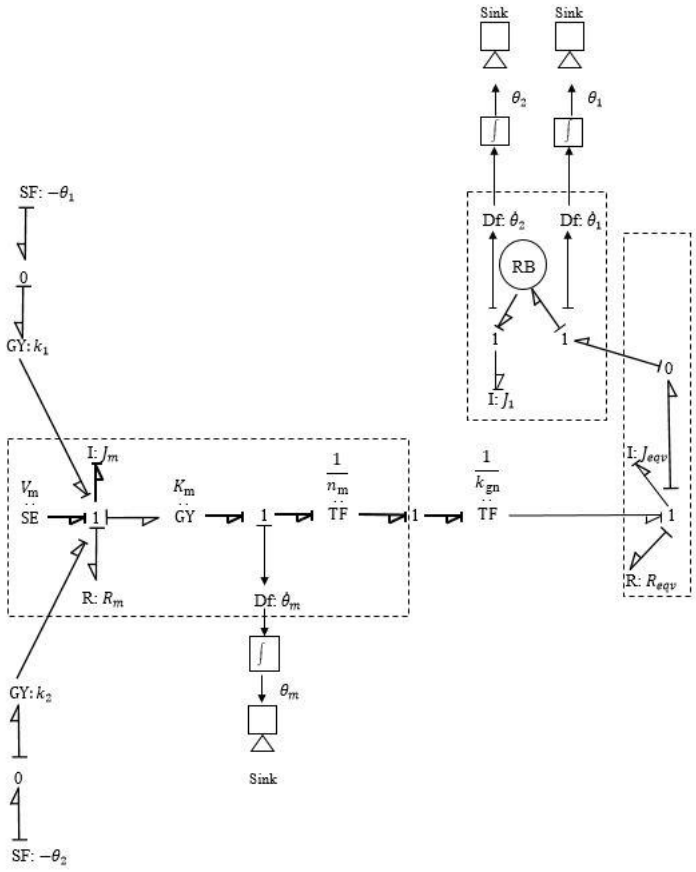

Fig. 5.2 Rayleigh beam model of single link flexible manipulator with full state feedback control using bond graph

In Section 3.2, the Rayleigh beam model of flexible manipulator has been discussed. Two models of single link flexible manipulator have been developed. The bond graph modelling has also been shown. Figure 3.9 shows the Rayleigh beam model of flexible manipulator using single Rayleigh beam element; this model was further refined for more accurate results using seven equal Rayleigh beam elements in series (Fig. 3.11). The states which were measured in single element model are rotation of the hub (θ_1) and the displacement of the tip of link (θ_2). In Fig. 5.2, the Rayleigh beam model using single Rayleigh beam element has been used for the application of full state feedback control. The single element model has been modified in such a way that every state can be sent as a feedback to their respective ports after getting multiplied by their corresponding gain values. The state variables θ_1 and θ_2 are measured using flow detector (sensors) represented as Df. These sensors detect the rate of change of these state vectors and

integrate it to give the corresponding values of displacement. These displacements are sent as negative feedback in form of source of flow Sf and are multiplied by their corresponding gain values $k_1$and k_2 at the gyrator (*GY*) to be converted as an effort input. These gain values have been calculated in Appendix III. These modified state values are then sent to the effort sum junction where the motor voltage is applied.

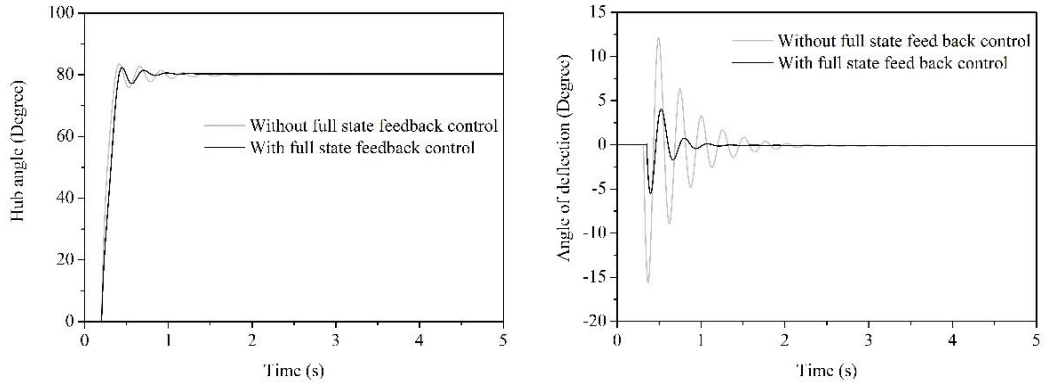

(a) (b)

Fig. 5.3 (a) Angle turned by servo motor and (b) Angle of deflection after using full state feedback controller on Rayleigh beam model of single element

The output and results of the Rayleigh beam model without the use of any control theory has been discussed in Section 3.2. The output results of the Rayleigh beam model represented by the grey line in Fig. 5.3 (a) and (b) are taken from Section 3.2. In Fig. 5.3 (a), the grey line indicates the Rayleigh beam model without the using the full state feedback control while, the solid black line represents the output of the Rayleigh beam model with the application of full state feedback control. It can be seen that the rise time of the Rayleigh beam model has slightly been increased after the use of full state feedback control. But, the settling time of the output has reduced along with slight reduction in the percent overshoot which was necessary to acquire a stable output. The steady state error has also been reduced; hence, in the controlled model, the hub rotation is almost equal to the desired angle of 80°. In Fig. 5.3 (b), the angle of deflection of the tip of the link is shown. It can be seen that the deflection in the tip is quite large when no control theory has been applied on the model. Also, the time period of vibration is approximately equal to 2.5s. But, when the full state feedback control theory is applied on the Rayleigh beam model, the state which represents this output has been controlled and the amplitude as well as the time period of vibration has been

reduced considerably. This control theory also satisfies the conditions of the performance parameters set in Table 5.1. Rise time, overshoot, maximum deflection and the input voltage are under the time domain values.

As discussed in Section 3.2.5, in order to achieve more accurate results, the Rayleigh beam model with single Rayleigh beam element was refined and a new model with seven Rayleigh beam elements was developed. This model was able to predict the experimental results more accurately as shown in Table 4.5. The states that have been controlled in the single Rayleigh beam element model are the same states which are controlled in the seven Rayleigh beam element model. The hub angle of rotation *i.e.* angle turned by the motor and the deflection at the tip of the link are the states to be controlled. In the single element model, the hub angle is measured from rotational port 1 and the deflection of the tip is given by the displacement measured from the rotational port 2 of the Rayleigh beam capsule (Sub-program) (Fig. 3.8). The seven element model is just addition of seven equal Rayleigh beam capsules in series. Each element has equal mass and length. Therefore, the rotational port 2 of every element will give the deflection taking place at the tip of that particular element which on summation will give the total deflection taking place in the link. The gains generated for single element model using the pole placement theory in Appendix III for hub angle rotation (θ_1) and deflection of the link *i.e.* displacement of rotational port 2 are used again in the seven element model. The gain obtained for the deflection of the link is used for the displacement of rotational port 2 of all the elements. Figure 5.4 shows the full state feedback control of seven Rayleigh beam element model.

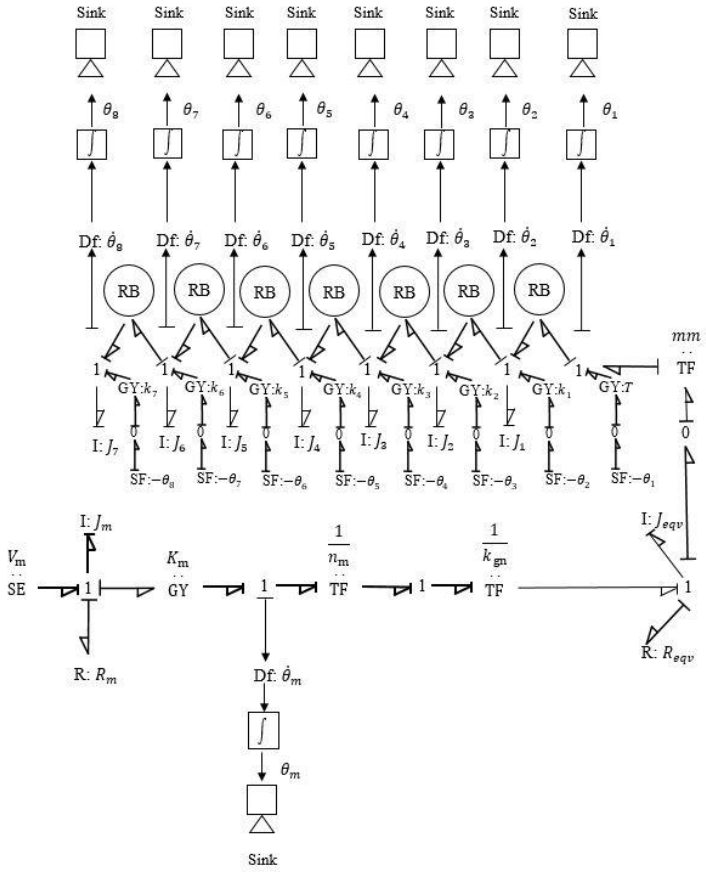

Fig. 5.4 Rayleigh beam model of seven Rayleigh beam element with full state feedback control

The Rayleigh beam model of seven Rayleigh beam element is discussed in Section 3.2.5. The seven element model has been modified in such a way that every state can be sent as a feedback to their respective ports after getting multiplied by their corresponding gain values. In this model, the displacements taking place at both the rotational ports of every element is measured using a flow detector (sensor) Df. This flow detector measures the rate of change of angular displacement and then integrates it to give the rotational displacement taking place at that port. This model was provided with a transformer modulus (mm) which works as a switch for transfer of motion when required. The feedback loop is connected after this transformer function so that the controller is not affected by its working. The displacements obtained from the rotational ports of every element are fed back to their respective ports. The gyrator (GY) function T represents the gain used for the angle of rotation of the hub whereas, the gyrator moduli k_1, k_2, k_3, k_4, k_5, k_6 and k_7 are the gains used for the deflection taking place at the tip of the link. In short, the displacements measured from each port of the

elements are sent as a negative feedback to their respective port after being multiplied by their corresponding gains. The results obtained from this control theory are shown in Fig. 5.5.

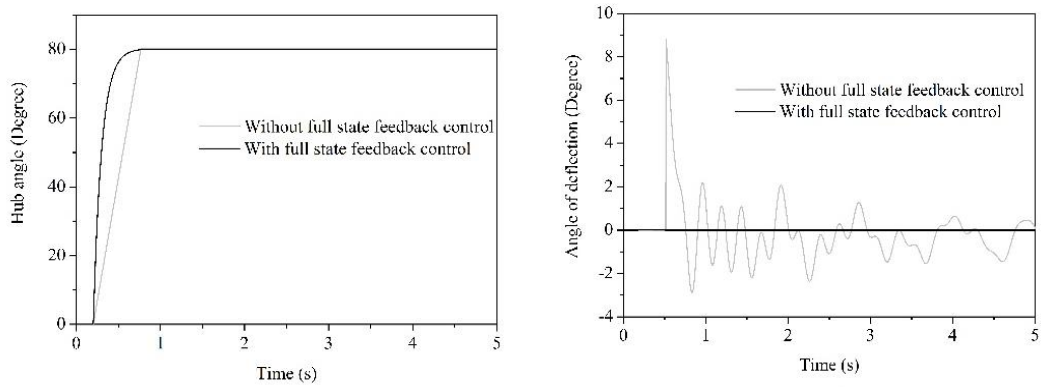

(a) (b)

Fig. 5.5 a) Angle turned by servo motor after and b) Angle of deflection after using full state feedback controller on Rayleigh beam model of seven element

In Fig. 5.5 (a), it can be seen that the Rayleigh beam model with seven Rayleigh beam elements shows hub rotation almost equal to the desired output of 80° without application of the full state feedback control theory. It can also be noted that the time domain requirements of the performance parameters mentioned in Section 5.1 is also satisfied. With the application of the feedback control, the result has been improved by the reduction in the rise time. This shows that the feedback control helps to reach the desired output faster than before with minimal effect on the other performance parameters. Figure 5.5 (b) shows the deflection that takes place at the tip of the link in Rayleigh beam model without feedback control and Rayleigh beam model with feedback control. It can be seen that the deflection is zero with the application of feedback control. This implies that the vibration that are induced in the link during the rotational motion is completely suppressed using the feedback control. It seems that the deflection of the tip has been controlled completely subdued but, deflection exists with very small amplitude. Figure 5.6 shows the deflection at the tip of the Rayleigh beam model with seven Rayleigh beam elements.

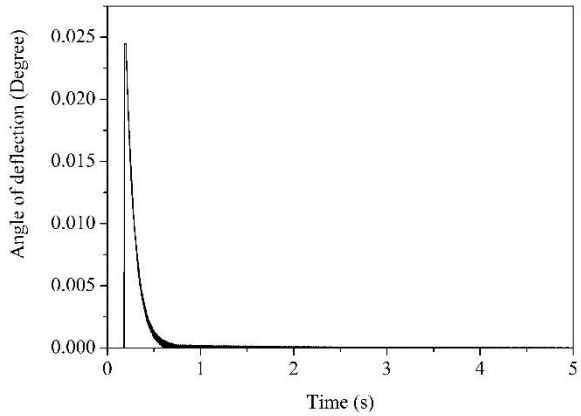

Fig. 5.6 Deflection at the tip of the Rayleigh beam model with seven Rayleigh beam elements

Thus, it can be concluded that deflection of the tip is not completely controlled but, the value of angular deflection is quite negligible.

5.3 LQR Control of Rayleigh Beam Model using Bond Graph

The pole placement method is quite effective and has an advantage that the system states can be controlled using the gain matrix. The poles of the system can be changed as per the desired system design requirements. This means that this method gives the freedom to alter the system performance according to the required closed loop characteristics. But, this method has major drawbacks. This method may generate the desired output but, does not develop a robust system. This means that if the system parameters are changed or some external disturbance is added, this model fails. This shows that the system will not be insensitive to the external disturbance if they exist. Another modern control theory which can help in generating the desired output from the system along with a guarantee of robustness is the linear quadratic regulator. In the LQR control theory, the poles of the system cannot be placed according to one's desire. The poles obtained from the LQR theory always guarantee robustness of the system but, the output obtained may not be exactly equal to the desired value. The difficulty in LQR control is to find the weights of the **Q** and **R** matrix for obtaining the desired output. The main objective of using the LQR theory is to control the states of the system to get as close as possible to the desired output without compromising the robustness of the system.

The objective function of linear quadratic regulator is given by

$$J = \int_0^\infty (\mathbf{x}^T\mathbf{Q}\mathbf{x} + \mathbf{u}^T\mathbf{R}\mathbf{u}) \tag{5.9}$$

where **R** and **Q** are square matrix and are symmetric in nature. **R** is known as the control cost matrix since it is used to tune the control input given to the system. **Q** is matrix which is used to modulate the states and hence, this is known as the state weighing matrix; it represents the transient energy. The optimal gains which will help to produce the required output without compromising the robustness of the system is given by

$$\mathbf{K} = \mathbf{R}^{-1}\mathbf{B}^T\mathbf{P} \tag{5.10}$$

where **K** is the gain matrix of size $1\times n$ and n is the number of states of the system, **B** is the input matrix of the system given in Eq. (5.3) and **P** is a positive definite unique solution obtained from the Riccati equation given by

$$\mathbf{P}\mathbf{A} + \mathbf{A}^T\mathbf{P} + \mathbf{Q} - \mathbf{P}\mathbf{B}\mathbf{R}^{-1}\mathbf{B}^T\mathbf{P} = \mathbf{0} \tag{5.11}$$

where **A** is the state coefficient matrix mentioned in Eq. (5.3). **Q** and **R,** are real matrix and positive definite in nature. The values in these matrices are entered manually and the closed loop performance of the system is observed. When the weights in the **R** matrix are increased the controller tries to stabilize the system with less energy and it is called as the expensive control strategy. If the values of the weights in **R** matrix are taken small, then the controller will not try to penalize the input and this is called as cheap control strategy. In short it can be concluded that if the weights in **Q** matrix are higher in value then the controller will aggressively try to bring the system back to zero irrespective of the amount of control input required and if the weights in **Q** matrix are smaller in value then the controller will behave conservatively by taking more time to control the states of the system. As the weights of the state is changed the gains obtained also vary. The system matrices of the Rayleigh beam model are mentioned in Appendix III. It can be seen that **A** matrix of the Rayleigh beam element is of the size 5×5 and therefore, the size of **Q** matrix will be 5×5. Since the number of inputs in the system is one, the **R** matrix will be of the size 1×1.

However, the weights in these matrices are selected randomly depending on the importance of states and control input. For the initial stage the **Q** matrix is taken as an identity matrix of 5×5 and **R** is taken as an identity matrix of size 1×1.

$$\mathbf{Q} = \begin{bmatrix} 1 & 0 & 0 & 0 & 0 \\ 0 & 1 & 0 & 0 & 0 \\ 0 & 0 & 1 & 0 & 0 \\ 0 & 0 & 0 & 1 & 0 \\ 0 & 0 & 0 & 0 & 1 \end{bmatrix} \tag{5.12}$$

$$\mathbf{R} = [1] \tag{5.13}$$

Using Eq. (5.9–5.13), the gains of the system are calculated. The gains of the Rayleigh beam model are calculated using the MATLAB function of LQR and are mentioned in Appendix IV. The last two gains are the gains generated are for the deflection of the tip of the beam and the angle turned by the hub. These gains obtained using the identity matrix of Eq. (5.12) and Eq. (5.13) do not produce the required closed loop response.

Now, since we know that the deflection in the beam and the hub angle are the states that are to be controlled, the weights corresponding to these states *i.e.* the last two rows of the **Q** matrix are altered. As seen during the pole placement method in Section 5.2, the Rayleigh beam model of seven Rayleigh beam elements is nothing but a cascade of seven Rayleigh beam elements in series. The gains generated for single element model were applicable on the seven element model and also produced better results (refer section 5.2). Therefore, the LQR optimal gains generated for the states of single element model will be used on the seven element model also. After certain number of trials, it was found that the following state weighing matrix given in Eq. (5.14) produce the desired output when applied on the Rayleigh beam model consisting of seven Rayleigh beam elements also satisfying the time domain requirements set in Table 5.1.

$$\mathbf{Q} = \begin{bmatrix} 1 & 0 & 0 & 0 & 0 \\ 0 & 1 & 0 & 0 & 0 \\ 0 & 0 & 1 & 0 & 0 \\ 0 & 0 & 0 & 2.5 & 0 \\ 0 & 0 & 0 & 0 & 0.001 \end{bmatrix} \tag{5.14}$$

MATLAB program used to generate these states are given in Appendix V. The LQR model of the Rayleigh beam theory using bond graph is shown in Fig. 5.7. The outputs measured are the hub angle of rotation and the deflection that takes place at the tip of the link. The gain generated for the hub angle (θ_1) is represented as T and the gain used for the tip deflection *i.e.* displacement of rotational port 2 (θ_i) where i = number of elements (refer Fig. 3.8) of each element are shown by k_1, k_2, k_3, k_4, k_5, k_6 and k_7.

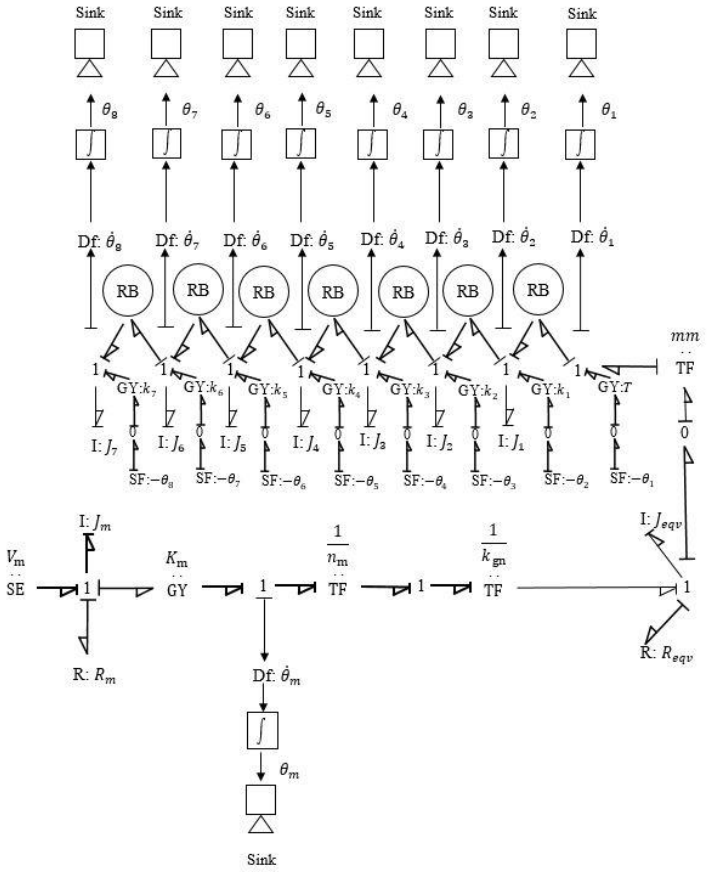

Fig. 5.7 Rayleigh beam model of single link flexible manipulator with LQR control using bond graph

The Rayleigh beam model of seven Rayleigh beam elements has been modelled and its working has been explained in Section 3.2.5. In Fig. 5.7, the seven element model has been modified in such a way that every state can be sent as a feedback to their respective ports after getting multiplied by their corresponding gain values. In this model the displacements taking place at both the rotational ports of every element is measured using a flow detector (Df). This flow detector measures the rate of change of angular displacement and then integrates it to give the rotational displacement taking place at that port. This model was provided a transformer moduli mm which works as a clutch for transfer of motion when required. The feedback loop is connected after this transformer function so that, the controller is not affected by its working. The displacements obtained from the rotational ports of every element are fed back to their respective ports as a negative feedback. The gyrator (GY) function T represents the gain used for the angle of rotation of the hub whereas, the gyrator moduli k_1, k_2, k_3, k_4, k_5, k_6 and k_7 are the gains used for the deflection taking place at the tip of the link. In short the displacements measured from each port of the elements are sent as a negative feedback to their respective port after being multiplied by their corresponding gains. The outputs obtained from the simulation are shown in Fig. 5.8 in comparison to the results which were obtained without the use of any control theory.

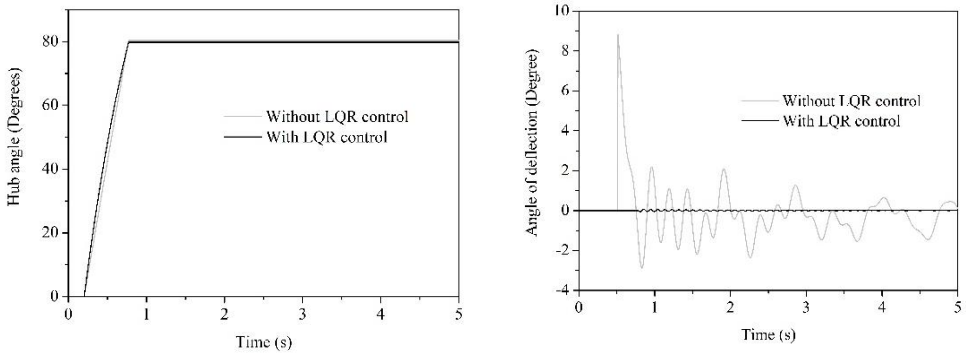

(a) (b)

Fig. 5.8 (a) Angle turned by servo motor and (b) Angle of deflection after using LQR on Rayleigh beam model

In Fig. 5.8 (a), the angle of rotation of the hub of the Rayleigh beam model without the use of any control theory is represented by the grey line while the LQR applied model is represented by the black line. The final steady state result is

approximately the same but, it is noticeable that there is a sudden acceleration in the rotation for few micro seconds and then a sudden deceleration is seen in the LQR applied system though the rise time is same. This shows that the motor rotates at a constant angular velocity when no control is applied on it and stops suddenly as soon as the source is turned off. Such sudden stoppage also plays a major role in imparting vibrations to the link. Whereas, in the LQR applied model it is seen that the angular velocity is not constant. It increases at the beginning and then decreases near the end time keeping the rise time constant. This prevents sudden stoppage of the motor and can help in reducing the vibrations that used to get induced due to sudden breakage. In Fig. 5.8 (b), the angle of deflection of the tip of the link is shown. The Rayleigh beam model with no control theory applied on it shows vibrations with amplitude more than 8°. The vibrations exist throughout the time of simulation. Whereas, the LQR applied system is quite stable in comparison to it. Vibration does exist but the amplitude is really small and the time period is also less. Figure 5.9 shows the vibrations in the link that exist in the LQR model. The amplitude of vibration is almost negligible. Hence the LQR theory is able to generate the desired outputs by controlling the required states.

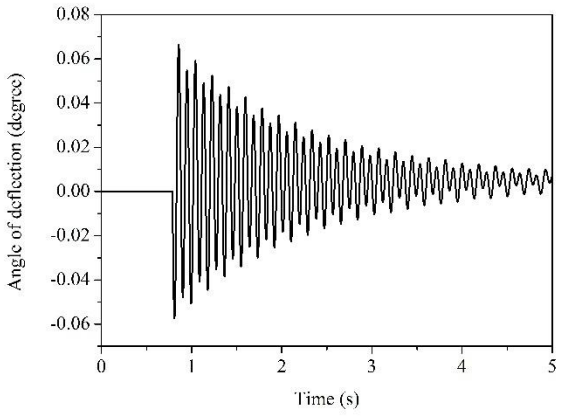

Fig. 5.9 Deflection of the tip of the link of LQR applied Rayleigh beam model

Table 5.2 Performance parameters of LQR applied Rayleigh beam model

Model Name	Control Technique	Rise Time (s)	Percent Overshoot (%)	Steady State Error (%)	Settling Time (s)	Maximum Deflection (°)
Rayleigh beam model	LQR	0.77	0	0.23	0.77	0.065

Table 5.2 shows the values of all the performance parameters of the Rayleigh beam model. The value of every parameter is within the pre-set desired values as mentioned in Table 5.1. The maximum deflection of the tip is mere 0.065° and it keeps decreasing from till the end of the simulation. The rise time is maintained constant at 0.77 s in both the models *i.e.* Rayleigh beam model with no control theory and the LQR model. The steady state error has reduced and the percent overshoot is still zero.

5.4 LQR Control of Model based on Lumped Parameter Method

Lumped parameter is another method to theoretically model a manipulator arm system. This method has been discussed in Section 3.1 for modelling a rotary flexible link. A system which has a flexible link mounted on to a servo motor through a hub and some gear train arrangement has been modelled in that section. The state space representation of the system is shown in Eqs. (3.33–3.38). The values of all the parameters used for the modelling are given in Table 3.1 and Table 4.1. The Simulink model is shown in Fig. 3.3 and its working has been explained. The MATLAB program to run the Simulink model is given in Appendix I. The outputs measured are, the angle rotated by the hub and the deflection that takes place at the tip of the link. The simulation results of this model have been given in Fig. 3.4. In Table 3.2, the performance parameters obtained from the simulation are stated. In Chapter 4, the outputs obtained from this dynamic model has been compared with the outputs of the dynamic model made using the Rayleigh beam theory and the outputs obtained from an actual manipulator arm system. A detailed comparison between both the models and the experiment, for all the performance parameter has been done in Table 4.3 and Table 4.5.

Since, the outputs obtained from the lumped model are not equal to the desired outputs, a control theory has to be applied on this model. Before the application of any

control theory the controllability and observability of the dynamic model is to be known. It is only possible to apply a control theory if the system is controllable and observable in nature and the controllability test procedure has been explained in detail in Section 5.1. The controllability of the lumped model is tested and the system is found controllable in Appendix II. In Section 5.3 the advantage of LQR control over full state feedback control has been explained. As the LQR control guarantees the robustness of the system for external disturbances and variations in system design parameters, it is a more preferable control technique than the full state feedback control. In Section 5.3, a LQR model of the Rayleigh beam theory has also been discussed and simulated. After application of the LQR control on the lumped model, both the dynamic models can be compared with respect to the outputs obtained and the performance parameters achieved. This will help in knowing which method is better for modelling a flexible manipulator system.

Figure 3.1 and 3.2 represent the lumped parameter model that has been considered for modelling and its schema diagram respectively. The equations of motions of this model have been derived in Section 3.1.3 and are given by Eq. (3.25) and Eq. (3.26). The control theory of linear quadratic regulator (LQR) has been explained in Section 5.3. The objective function is given by

$$J = \int_0^\infty (\mathbf{x}^T \mathbf{Q} \mathbf{x} + \mathbf{u}^T \mathbf{R} \mathbf{u}) \tag{5.15}$$

where **Q** is the state coefficient matrix and **R** is the control cost matrix. **x** represents the states of the system and **u** represents the control input to the system. The optimum solution of the system is obtained by

$$\mathbf{K} = \mathbf{R}^{-1} \mathbf{B}^T \mathbf{P} \tag{5.16}$$

where **K** is the gain matrix of size $1 \times n$ and n is the number of states of the system, **B** is the input matrix stated in Eq. (3.29) and **P** is the positive definite unique solution obtained from the Riccati equation given by

$$\mathbf{P}\mathbf{A} + \mathbf{A}^T \mathbf{P} + \mathbf{Q} - \mathbf{P}\mathbf{B}\mathbf{R}^{-1}\mathbf{B}^T \mathbf{P} = \mathbf{0} \tag{5.17}$$

where **A** is the state coefficient matrix mentioned in Eq. (3.29). **Q** and **R,** are real matrix and positive definite in nature. The values in these matrices are entered manually and the closed loop performance of the system is observed. When the weights in the **R** matrix are increased the controller tries to stabilize the system with less energy and it is called as the expensive control strategy. If the values of the weights in **R** matrix are taken small, then the controller will not try to penalize the input and this is called as cheap control strategy. In short it can be concluded that if the weights in **Q** matrix are higher in value then the controller will aggressively try to bring the system back to zero irrespective of the amount of control input required and if the weights in **Q** matrix are smaller in value then the controller will behave conservatively by taking more time to control the states of the system. As the weights of the state are changed the gains obtained also vary. The system matrices of the lumped parameter model are mentioned in Appendix I. It can be seen that **A** matrix of the is of the size 4×4 and therefore, the size of **Q** matrix will be 4×4. Since the number of inputs in the system is one, the **R** matrix will be of the size 1×1.

$$\mathbf{A}=\begin{bmatrix} 0 & 0 & 1 & 0 \\ 0 & 0 & 0 & 1 \\ 0 & K_s / J_{eqv} & -R_{eqv} / J_{eqv} & 0 \\ 0 & -K_s(J_s + J_{eqv}) / J_s J_{eqv} & B_{eqv} / J_{eqv} & 0 \end{bmatrix} \tag{5.18}$$

$$\mathbf{B}=\begin{bmatrix} 0 \\ 0 \\ 1/J_{eqv} \\ -1/J_{eqv} \end{bmatrix} \tag{5.19}$$

However, the weights **Q** and **R** matrices are selected randomly depending on the importance of states and control input. For the initial stage the **Q** matrix is taken as an identity matrix of 4×4 and **R** is taken as an identity matrix of size 1×1.

$$\mathbf{Q}=\begin{bmatrix} 1 & 0 & 0 & 0 \\ 0 & 1 & 0 & 0 \\ 0 & 0 & 1 & 0 \\ 0 & 0 & 0 & 1 \end{bmatrix} \tag{5.20}$$

$$\mathbf{R} = [1] \tag{5.21}$$

Using Eq. (5.15 – 5.21), the gains of the system are calculated. The gains of the lumped parameter model are calculated using MATLAB function of LQR and are mentioned in Appendix VI. These gains obtained using the identity matrix of Eq. (5.20) and Eq. (5.21) do not produce the required closed loop response. The states of the system mentioned in Eq. (3.31) are

$$x^T = [\theta \ \alpha \ \dot{\theta} \ \dot{\alpha}] \tag{5.22}$$

Now, **Q** = diagonal$\begin{bmatrix} q_1 & q_2 & q_3 & q_4 \end{bmatrix}$ and the gain matrix **K** = $\begin{bmatrix} k_1 & k_2 & k_3 & k_4 \end{bmatrix}$, by varying q_i independently the effects on the state variables being measured were observed. When, the weights of the state weighing matrix were changed the following observations were made

- Increasing the value of q_1 increases the gain related to the servo motor angle *i.e.* k_1. This decreases the settling time and the peak of overshoot.
- Change in the value of q_2 does not affect the performance parameters much.
- Increasing the value of q_3 increases the gain related to the angular velocity of the motor *i.e.* k_4. This slows down the rotation of the motor.
- Increase in the value of q_4 decreases k_2 and k_4. It minimizes the link deflection without affecting the states related to servo motor rotation.

After many trials, the state weighting matrices which yield adequate output results were obtained and are

$$\mathbf{Q} = \begin{bmatrix} 150 & 0 & 0 & 0 \\ 0 & 1 & 0 & 0 \\ 0 & 0 & 1 & 0 \\ 0 & 0 & 0 & 3 \end{bmatrix} \tag{5.23}$$

$$\mathbf{R} = [1] \tag{5.24}$$

The Simulink model developed for LQR control of the lumped parameter model is give in Fig. 5.10. The MATLAB program used to run the model is given in Appendix VI.

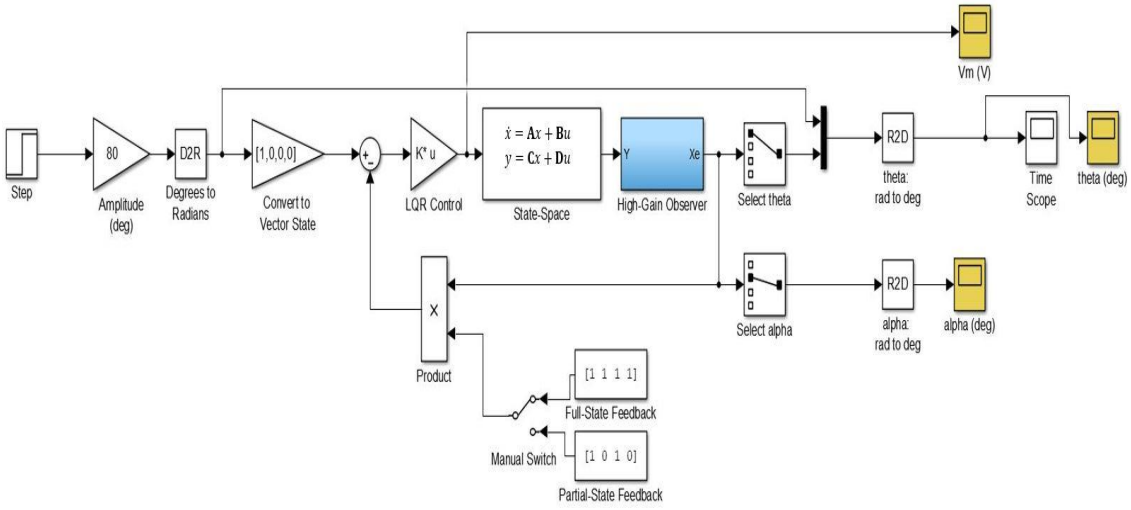

Fig. 5.10 Simulink model for LQR control of lumped parameter model

A step input is applied using a source block from the Simulink library. The time period and initial conditions of the input can be set within the block. A gain block is used to set the amplitude of the step input to 80° which is the desired angular rotation. D2R block converts the value from degrees to radian. Since the feedback gain matrix is of the size 1×4, the input has to be converted to the same size. Therefore, a gain block with value [1, 0, 0, 0] is added. The input and the feedback of the state variables meet at the summing junction and are sent forward to the LQR gain block. Every state is multiplied by its corresponding gain value and are sent to the plant represented by the state space. High gain observers are used to observe the states which are to be controlled. The states are given in Eq. (5.22). The four states observed are then sent back as a feedback where they again get multiplied by their respective gain values. The selector block is used to select the output states which are to be displayed. The two output variables selected are the angle of rotation of the motor (θ) and angle of deflection taking place at the tip of the link (α). The output results obtained are shown in Fig. 5.11

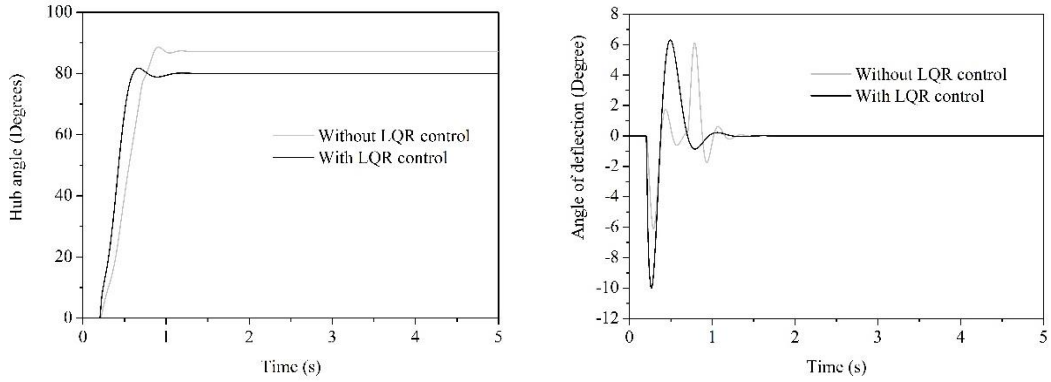

(a) (b)

Fig. 5.11 (a) Angle turned by servo motor and (b) Angle of deflection after using LQR on Lumped parameter model

It can be seen from Fig. 5.11 (a) that the angle turned by the servo motor *i.e.* angle turned by the hub in the LQR applied lumped parameter model, represented by the black line is exactly equal to 80° which is the desired output. The steady state error has reached zero after application of LQR control. The rise time of the system has decreased compared to the model which had no control theory applied on it. The percent overshoot has increased by a small magnitude after the application of the LQR control but the desired output has been achieved accurately. In Fig. 5.10 (b), the deflection of the tip of the link has been mapped. The vibrations induced in the link after the application of the LQR theory is less compared to the uncontrolled model. The time period of vibration has also reduced. But, the maximum deflection of the link has increased in magnitude. This deflection can be changed with the modification of the **Q** matrix. Further attempts and study can be done on what values of the weighing matrix the link deflection can be achieved minimum.

Table 5.3 Performance parameters of LQR applied lumped parameter model

Model Name	**Control Technique**	**Rise Time (s)**	**Percent Overshoot (%)**	**Steady State Error (%)**	**Settling Time (s)**	**Maximum Deflection (°)**
Lumped parameter model	LQR	0.60	2.13	0	1.64	9.99 (negative)

Table 5.3 shows that all the time domain requirements of the performance parameters given in Table 5.1 is satisfied by the LQR applied model but, the maximum

deflection that takes place in the link is more quite large than the Rayleigh beam model. The steady state error has reached an absolute zero value and the rise time has also reduced. Settling time of the output has also reduced compared to the lumped model which had no control theory applied on it. Further attempts can be made to achieve better results.

5.5 Flexible Manipulator with LQR Control

In Chapter 3, two dynamic models of a flexible manipulator system consisting of a single flexible link, has been modelled. These two models were then compared with each other at the end of the chapter. The comparison of the outputs measured and the performance parameters obtained has been stated in Table 3.4. In order to find out how accurately these models can predict the output of a real flexible manipulator system, an experimental setup has been discussed in Chapter 4. The dimensions of the link and the parameters which were used to design this test setup have been mention in Table 4.1 and Table 4.2. The components used and their nomenclature has been given in detail in Section 4.2. Figure 4.2 shows every element of the flexible manipulator system according to its nomenclature. The sensors used in measuring the required outputs and the working principle of the manipulator system has been explained in Section 4.3 with the help of the Simulink model developed to run the system. A data acquisition card and an amplifier are present between the hardware and the software for transfer of data and amplification of input and output signals.

Table 5.4 Performance parameters of flexible manipulator

Method	Rise time (s)	Percent overshoot (%)	Steady state error (%)	Settling time (s)	Maximum deflection (°)
Flexible manipulator	0.81	4.27	2.11	2.40	8.58 (negative)

The following are the performance parameters obtained from the flexible manipulator during experimentation in Section 4.4. In comparison to the time domain requirements stated in Table 5.1, it can be seen that the steady state error in the output is high as well as the maximum deflection value is more than the permissible limit.

Therefore, this system has to be controlled using a controller which can control the required states. It has been mentioned in Chapter 3 that the two main states that are to be controlled are the hub angle of rotation and the deflection of the tip of the link. The LQR controlled dynamic model of both lumped parameter method and Rayleigh beam theory has been developed in Section 5.4 and Section 5.3 respectively. The gains generated by these models can be implemented on the experimental setup.

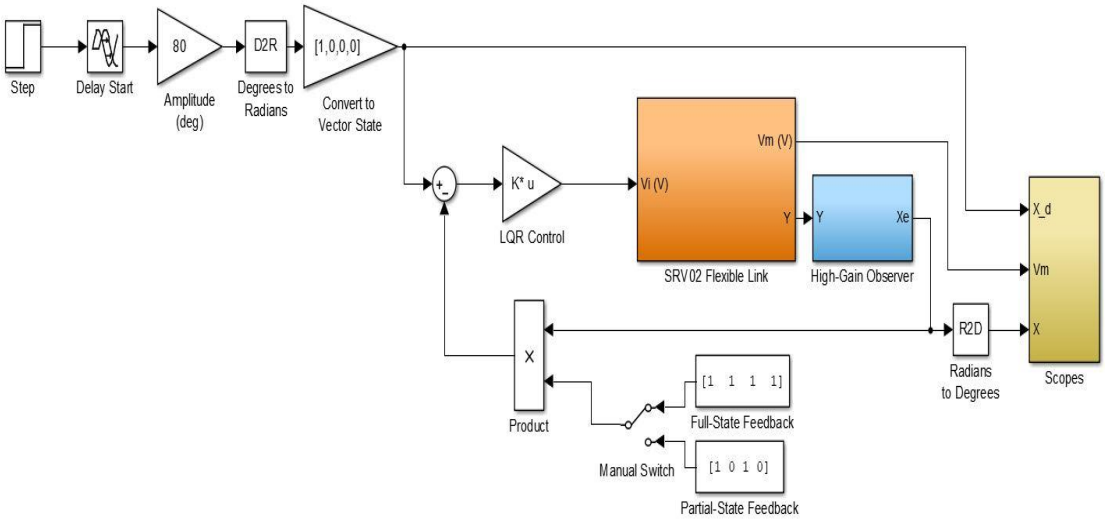

Fig. 5.12 Simulink model of flexible manipulator with LQR control

In this chapter, LQR control is implemented on the experimental setup using the gains generated from LQR applied lumped parameter model. By measuring all the states that have been mentioned in Eq. (5.22) and taking feedback of the values that have been obtained, the corresponding gains can be multiplied to their states. These gains are loaded into the MATLAB program which runs the Simulink model of this experimental setup. In Fig. 5.12, it can be seen that the state space block of the LQR applied lumped parameter model shown in Fig. 5.10 has been replaced by the manipulator arm setup. A step input is applied using a source block from the Simulink library. The time period and initial conditions of the input can be set within the block. The next block connected is the transport delay block. It is used to delay the input by a certain specified time period *i.e.* the amount of time during the simulation when the input signal is delayed from being propagated to the output. It is helpful in cases where the real system has elements which does not give an output as soon as the input is applied *e.g.* pumps, motors *etc.* A gain block is used to set the amplitude of the step

input to 80° which is the desired angular rotation. The D2R block converts the value from degrees to radian. The feedback of only four states of the system is measured using the sensors. Therefore, the gain matrix is of the size 1×4. Since the feedback gain matrix is of the size 1×4, the input has to be converted to the same size. Therefore, a gain block with value [1, 0, 0, 0] is added. The input and the feedback of the state variables meet at the summing junction and are sent forward to the LQR gain block. Every state is multiplied by its corresponding gain value and is sent to the plant represented by the SRV02 Flexible Link. High gain observers are used to observe the states which are to be controlled. The two states *i.e.* the angle of rotation of the hub (θ) and the deflection at the tip of the link (α) are measured using an optical encoder and a strain gauge. Derivative of these measured values are then taken to obtain the other two state values. The four states observed are then sent as a feedback where they again get multiplied by their respective gain values. The selector block is used to select the output states which are to be displayed. The two output variables selected are the angle of rotation of the motor (θ) and angle of deflection taking place at the tip of the link (α). The output results obtained are shown in Fig. 5.13.

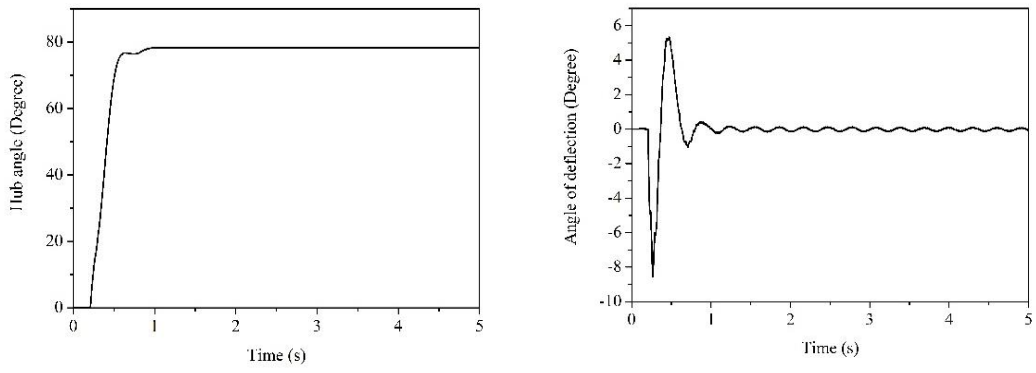

(a) (b)

Fig. 5.13 (a) Angle turned by servo motor and (b) Angle of deflection of the link using LQR control

In Fig. 5.13(a), it can be seen that the experimental setup does not give better result than the theoretical model made using lumped parameter method. The overshoot has been recorded zero during the experimentation but the steady state error is obtained which was absent in the theoretical model. The rise time is almost equal to the theoretical model and the settling time is slightly less. Figure 5.13 (b) shows that the

maximum deflection predicted by the lumped model is almost the same. But the theoretical model predicts that the vibrations extinct after few micro seconds during the experimentation whereas, in the real case vibrations still persists in the link.

Table 5.5 Performance parameter of LQR controlled flexible manipulator

Model Name	Control Technique	Rise Time (s)	Percent Overshoot (%)	Steady State Error (%)	Settling Time (s)	Maximum Deflection (°)
Single link flexible manipulator	LQR	0.62	0	2.1102	1.24	8.54 (negative)

In Fig. 5.14, the outputs from the LQR controlled Rayleigh beam model, LQR controlled lumped parameter model and LQR controlled flexible manipulator are shown. The black dashed line represents the out of the lumped parameter model. The solid black line represents the output of the Rayleigh beam model and the grey line shows the output obtained from the experimentation of flexible manipulator. The outputs shown are the hub angle of rotation and the angle of deflection of the tip of the link. The performance parameters that can be observed from the results are shown in Table 5.6.

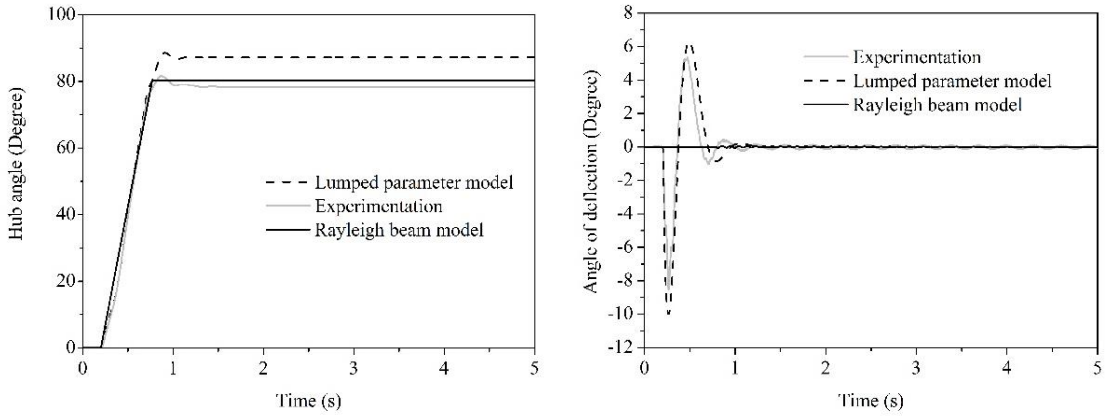

(a) (b)

Fig. 5.14 (a) Comparison of angle turned by the servo motor and
(b) Comparison of angle of deflection of the link after the application of LQR control

In Table 5.6, a comparison of all the methods is made. The comparison is namely done between the LQR controlled Rayleigh beam model, LQR controlled lumped parameter model and LQR controlled flexible manipulator system. It can be seen that, the maximum deflection is the least in the Rayleigh beam model and the maximum in the lumped parameter model. The settling time is also least in the Rayleigh beam model and the maximum in the lumped parameter model. The steady state error is predicted zero by the lumped parameter model but, a steady state error of 2.11% exists in the flexible manipulator system. The rise time predicted by the Rayleigh beam model is the highest. The percent overshoot in the Rayleigh beam model and the flexible manipulator is zero.

Table 5.6 Comparison of performance parameters

Model Name	**Control Technique**	**Rise Time (s)**	**Percent Overshoot (%)**	**Steady State Error (%)**	**Settling Time (s)**	**Maximum Deflection (°)**
Rayleigh beam model	LQR	0.77	0	0.23	0.77	0.065
Single link flexible manipulator	LQR	0.62	0	2.11	1.24	8.54 (negative)
Lumped parameter model	LQR	0.60	2.13	0	1.64	9.99 (negative)

Chapter 6 Conclusions and Scope of Future Work

6.1 Conclusions

In Chapter 3, two distinct methods to develop a dynamic model of a manipulator system consisting of a single flexible arm were discussed. The angle rotated by the hub *i.e.* the angle turned by the servo motor for a given input was one of the output that was measured. The second output measured was the deflection of the tip of the link. After comparing the results of both the models, it was noted that the Rayleigh beam model recorded less vibrations in comparison to the lumped parameter model. The steady state error and the percent overshoot were also less than the lumped model. After experimentation of a real hardware setup of flexible manipulator in Chapter 4, it was observed that the results obtained from the Rayleigh beam model were closer compared to the results obtained from the lumped model. The detailed discussion is given at the end of Chapter 4. This concludes that the Rayleigh beam theory is a better method to develop the dynamic model of a flexible manipulator. The results obtained from the LQR applied Rayleigh beam model is very close to the desired output and also satisfies the time domain requirements stated in Chapter 5. Therefore, it can be concluded that if the same number of states of the flexible manipulator are measured using some sensors and are multiplied by the corresponding gains generated by the Rayleigh beam model, the flexible manipulator might give output closer to the desired results.

6.2 Future scopes

Though after allot of efforts a dynamic model of the flexible link manipulator has been developed using the Rayleigh beam theory this model can be improved in future and the following progress can be made

- A Rayleigh beam model consisting of more number of Rayleigh beam elements can be developed which will help to record the end point deflection of the link more accurately.
- The Rayleigh beam model developed can be compared with other famous methods like finite element and assumed mode method.
- Modern controllers other than pole placement and LQR can be applied on the Rayleigh beam model to know whether better results can be achieved.

- Implementation of the Rayleigh beam model with LQR control theory on the actual flexible manipulator test setup can be done.
- The Rayleigh beam model developed for single link can be further extended for two link and three link models *i.e.* multilink system.

References

A. De Luca and B. Siciliano. Regulation of flexible arms under gravity. *IEEE transactions on Robotics and Automation*, 9(4), pp. 463–467, 1993

A. Deluca and B. Siciliano. Closed-form dynamic model of planar multilink lightweight robots. *IEEE Transaction on Systems, Man and Cybernetics*, 21(4), pp. 826–839, 1991

A. Green and J. Z. Sasaidek. Dynamics and trajectory control of a two-link robot manipulator. *Journal of Vibrations and Control*, Volume 10, pp. 1415–1440, 2004

A. Konno and M. Uchiyama. Modelling of a flexible manipulator dynamics based upon holzer model. *In proceedings of the IEEE/ RSJ International Conference on Intelligent Robots and Systems (IROS-96)*, Volume 1, pp. 223–229, 1996

A. Konno, L. Deman and M. Uchiyama. A singularly perturbed method for pole assignment control of flexible manipulator. *Robotica*, 20(6), pp. 637–651, 2002

A. Mukherjee, R. Karmarkar and A. K. Samantary, Bond Graph in Modelling, Simulation and Fault Identification, 2006

A. S. Morris and A. Madani. Computed torque control applied to a simulated two flexible link robot. *Transaction of Institute of Measurement and Control*, 19(1), pp. 50–60, 1997

A. Singla, A. Tiwari and B. Dasgupta. Command shaped close loop control of flexible robotic manipulator. *Journal of Vibration Engineering and Technologies*, 4(2), 2016

A. Singla, A. Tiwari and B. Dasgupta. Vibration suppression during input tracking of a flexible manipulator using command shaping. *Indian Academy of Sciences*, 40(6), 2015

B. P. Nagaraj, B. S. Nataraju and D. N. Chandrashekar. Non-dimensional parameters for the dynamics of a single flexible link. *In International Conference on Theoretical, Applied, Computational and Experimental Mechanics(ICTACEM)*, 2001

D. G. Wilson, R. D. Robinett, G. G. Parker, and G. P. Starr. Augumented sliding mode control for flexible link manipulator. *Journal of Intelligent and Robotic Systems*, Volume 34, pp. 415–430, 2002

D. Karnopp. Bond graph models of electrochemical energy storage: electrical, chemical and thermal effects. *Journal of Franklin Institute*, 327(6), pp. 983–992, 1990

D. W. Roberts, D. J. Balance, and P. J. Gawthrop. Design and implementation of bond graph observer for robot control. *Control Eng. Practice,* 3(10), pp. 1447–1457, 1995

D. Wang and M. Vidyasagar. Modelling a class of multilink manipulators with last link flexible. *IEEE Transaction on Robotics and Automation*, 8(1), pp. 33–41, 1992

De Luca and Siciliano. Trajectory control of a nonlinear one link flexible arm. *International journal of control*, 50(5), pp.1699–1715, 1989

F. Rakhsha and A. Goldenberg. Dynamics modelling of single link flexible robot. *Proceedings of IEEE International Conference on Robotics and Automation*, Volume 2, pp. 984–989, 1985

G. D. Tanguy, A. Rahmani, and C. Sueur. Bond graph aided design of controlled systems. *Simulations Practice and Theory*, pp. 493–513, 1999.

G. Hastings and W. Book. Verification of a linear dynamic model for a flexible robotic manipulator. *IEEE Control Systems Magazine*, 7(1), pp. 61–64, 1987

G. S. Kiran, A. Kumar, P. M. Pathak, and N. Sukavanam. Trajactory control of flexible space robot. *Proceedings of IEEE International Conference on Mechatronics and Automation*, 2008

G. Zhu, S. S. Ge, and T. H. Lee. Simulation studies of tip tracking control of a single link flexible robot based on a lumped model. *Robotica*, 17(1), pp. 71–78, 1999

H. B. Pacejka. Modelling complex vehicle system using bond graphs. *Journal of Franklin Institute*, 319(1/2), pp. 67–81, 1985

H. C. Moulin and E. Bayo. Accuracy of discrete models for the inverse dynamics of flexible arms, feasible trajectories. *In Proceedings of the 29th IEEE Conference on Decision and Control*, pp. 531–532, 1990

H. Geniele, R. V. Patel and K. Khorasani. End-point control of flexible manipulator: theory and experiments. *IEEE Transactions on Control Systems Technology*, 5(6), pp. 556–570, 1997

H. Moulin and E. Bayo. On the accuracy of the end-point trajectory tracking for a flexible arm by noncasual inverse dynamics. *ASME Journal of Dynamic Systems, Measurement, and Control*, 113, pp. 320–324, 1991

H. S. Tzou. Nonlinear structural dynamics of space manipulators with elastic joints. *International Journal of Analytical and Experimental Modal Analysis*, 4, pp. 117–123, 1989

Instructor Workbook Flexible Link Experiment for Matlab®/Simulink® Users

J. D. Lee and B. L. Wang. Optimal control of a flexible robot arm. *Computers & Stuctures*, 29(3), pp. 459–467, 1988

J. Vaughan, A. Yano and W. Singhose. Comparison of robust input shapers. *Journal of Sound and Vibration*, 315, pp. 797–815, 2008

K. Krishnamurthy. Dynamic modelling of a flexible cylindrical manipulator. *Journal of Sound and Vibration*, 132(1), pp. 143–154, 1989

K. W. Buffinton and T.R. Kane. Dynamics of a beam moving over supports. *International Journal of Solids and Structures*, 21(7), pp. 617–643, 1985

L. Lanari and J. T. Wen. Asymptotically stable set point control laws for flexible robot. *Systems & Control letters*, 19(2), pp. 119–129, 1992

M. Benosman and G. Le Vey. Control of flexible manipulators: A survey. *Robotica*, 22(5), pp. 533–545, 2004

M. Khairudin, Z. Mohamed, and A.R. Husain. Dynamic model and robust control of flexible link robot manipulator. *Telkomnika*, 9(2), 2011

M. Uchiyama, A. Konno, T. Uchiyama and S. Kanda. Development of a flexible dual arm manipulator testbed for space robotics. *In Proceedings of IEEE international Workshop on Intelligent Robots and System IROS'90, 'Towards a New Frontier Application'*, pp. 375–381, 1990

Mingli bai, Dong Hua Zhou and Helmut Schwarz. Adaptive augmented state feedback control for an experimental planar two-link flexible manipulator. *IEEE Transactions on Robotics and Automation*, 14(6), 1998

P. B. Usoro, R. Nadira and S.S. Mahil. A finite element/ lagrange approach to modelling lightweight flexible manipulators. *Journal of Dynamic System, Measurement, and Control*, Volume 108, pp. 198–205, 1986

P. J. Gawthrop. Bond graphs: A representation of mechatronic systems. *Mechatronics*, 1(2), pp. 127–156, 1991

R. H. Cannon and E. Schmitz. Initial experiments on end point control of a flexible one link robot. *International Journal of Robotics and Research* 3(3), pp. 62–75, 1984

R. J. Theodore and A. Ghosal. Comparison of assumed mode method and finite element model for flexible multilink manipulator. *International Journal of Robotics Research*, 14(2), pp. 91–111, 1995

R. J. Theodore and A. Ghosal. Modelling of a flexible link manipulator with prismatic joints. *IEEE Transaction on System, Man, and Cybernetics, part B: Cybernetics*, 27(2), pp.296–305, 1997

S. Kumar, S. Kumar, and C.D. Singh. Modeling and simulation of underwater flexible manipulator as Rayleigh beam using bond graph. *International Journal of Mechanical and Mechatronics Engineering*, 9(8), 2015

T. K. Bera, A. K. Samantaray, and R. Karmakar. Bond graph modelling of planar prismatic joints. *Mechanisms and Machine Theory*, Volume 49, pp. 2–20, 2012

T. Singh. Dynamics and control of a flexible arm robots. Ph.D. Thesis, Mechanical Engineering, Waterloo University, Canada, 1991

T. Yoshjkawa and K. Hosoda. Modelling of flexible manipulators using virtual rigid links and passive joints. *International Journals of Robotics Research*. 15(3), pp. 290–299, 1996

V. A Utkin. Control of elastic multilink manipulator based on dynamic compensation method. *In proceedings of IEEE International Symposium on Circuits and Systems (ISCAS'98)*, 6, pp. 594–597, 1998

W. J. Book. Analysis of massless elastic chains with servo controlled joints. *ASME Journal of Dynamic System, and Control*, 101, pp. 187–192, 1979

W. Khalil and M. Gautier. Modelling of mechanical system with lumped elasticity. *In Proceedings of IEEE International Conference on Robotica and Automation*, 4, pp. 3964–3969, 2000

Z. Mohammad and M. O. Tokhi. Command shaping techniques for vibration control of a flexible robot manipulator. *Mechatronics*, 14(1), pp. 69–90, 2004

Appendix-I

```
%% This program shows the simulation program of the dynamic model made using
lumped parameter model
%The parameters of the system used for dynamic modelling are listed
clc;
clear all;
Ks= 1.3000;
Jeq= 9.76*10^(-5);
Js=0.0038274;
Req=0.01500;
Rm=2.6000;
kt=0.0077;
km=0.0077;
Kg=70;
eta_g=0.9000;
eta_m=0.6900;

%% State Space Representation
% The state space representation is shown
A=[0 0 1 0
  0 0 0 1
  0 Ks/Jeq -Req/Jeq 0
  0 -Ks*(Jeq+Js)/Jeq/Js Req/Jeq 0];
B= [0
      0
   1/Jeq
   -1/Jeq];
eig (A)
C= [1 0 0 0
     0 1 0 0]
 D= [0 0]'

 %% Actuator dyanmics added to the state space model
 % This part adds the motor dynamics given in Eq. (3.9) to the state space
 % model of the flexible manipulator
Ao = A;
Bo = B;
B = eta_g*Kg*eta_m*kt/Rm*Bo
A(3,3) = Ao(3,3) - Bo(3)*eta_g*Kg^2*eta_m*kt*km/Rm
A(4,3)= Ao(4,3) -Bo(4)*eta_g*Kg^2*eta_m*kt*km/Rm
```

Appendix-II

A.II.I

%% This program checks the controllability and observability of the dynamic model made using lumped parameter model

```
clc;
clear all;
Ks= 1.3000;
Jeq = 9.76*10^(-5);
Js =0.0038274;
Req =0.01500;
Rm=2.6000;
kt =0.0077;
km=0.0077;
Kg=70;
eta_g=0.9000;
eta_m=0.6900;

%% State Space Representation
% The state space representation is shown

A=[0 0 1 0
   0 0 0 1
   0 Ks/Jeq -Req/Jeq 0
   0 -Ks*(Jeq+Js)/Jeq/Js Req/Jeq 0];
B= [0
       0
    1/Jeq
    -1/Jeq];
eig (A)
C= [1 0 0 0
      0 1 0 0]
 D= [0 0]'

 %% Actuator dyanmics added to the state space model
 % This part adds the motor dynamics given in Eq. (3.9) to the state space
 % model of the flexible manipulator

Ao = A;
Bo = B;
B = eta_g*Kg*eta_m*kt/Rm*Bo
A(3,3)= Ao(3,3) - Bo(3)*eta_g*Kg^2*eta_m*kt*km/Rm
A(4,3) = Ao(4,3) - Bo(4)*eta_g*Kg^2*eta_m*kt*km/Rm

%% Order, Rank, Controllability and Observability of the syatem
% This part checks whether the system is controllable or not. If the rank
% of the controllablity matrix is equal to the order of the system then the
% system is controllable
```

```
sys= ss(A,B,C,D);
sys_order= order(sys)
sys_rank= rank(ctrb(sys))
Ob = obsv(sys)
Ctrb = ctrb(sys)
```

A.II.II

% The controllability of the Rayleigh beam model has been checked in the control pad module of the software SYMBOLS Shakti. The syntax used to know the controllability is

T= ACONB <ENTER>
RANK(T) <ENTER>

```
(A)=
 -1.37692579   0.          -13.4024539  -1.3080795   -0.65403975
  0.          -14444.4444  -3420.59016   0.           0.
 -0.688462895  1854.72     -180.493432  -0.65403975  -1.3080795
  526.315789   0.           0.           0.           0.
  0.           0.           10245.9016   0.           0.
(B)=
  0.
  1.
  0.
  0.
  0.
(C)=
  526.315789   0.           0.           0.           0.
  0.           0.           10245.9016   0.           0.
  0.           0.           10245.9016   0.           0.
  0.           0.           445389.344   0.           0.
(D)=
  0.
  0.
  0.
  0.
>T=CONMAT(p)
>T
    0.           0.          -24857.7993   351149098   -4.912e+012
    1.          -14444.4444   202297738   -2.829e+012   3.9567e+016
    0.           1854.72     -27125164.8   3.8007e+011 -5.315e+015
    0.           0.           0.          -13083052.3   1.8481e+011
    0.           0.           19003278.7  -2.779e+011   3.8942e+015
>RANK(T)
   5
>ACONB
  System is controllable !
```

Fig. A.1 Controllability test [**Symbols-Shakti BondPad Version 2.0, High Tech Consultants**]

Appendix-III

%% This program produces full state feedback control gains for Rayleigh beam model with single Rayleigh beam element

```
clc;
clear all;
A= [-1.37693 0 -13.4025 -1.30808 -0.65404;0 -14444.4 -3420.59 0 0;
-0.688463 1854.72 -180.493 -0.65404 -1.30808;
526.316 0 0 0 0;
```

```
0 0 10245.9 0 0];
B= [0;1;0;0;0];
C= [526.316 0 0 0 0;0 0 10245.9 0 0;
0 0 10245.9 0 0;
0 0 445389 0 0];
D= [0;0;0;0];

P = 1.0e+04 *[-1.3982 + 0.0000i;
                    -0.0732 + 0.0000i;
                    -0.0008 + 0.0023i;
                     -0.0008 - 0.0023i;
                     -0.0011 + 0.0000i];

K2= place (A, B, P)
```

Appendix-IV

%% This program produces LQR control gains for Rayleigh beam model with single Rayleigh beam element using identity **Q** matrix

```
clc;
clear all;
A= [-1.37693 0 -13.4025 -1.30808 -0.65404;0 -14444.4 -3420.59 0 0;
-0.688463 1854.72 -180.493 -0.65404 -1.30808;
526.316 0 0 0 0;
0 0 10245.9 0 0];
B= [0;1;0;0;0];
C= [526.316 0 0 0 0;0 0 10245.9 0 0;
0 0 10245.9 0 0;
0 0 445389 0 0];
D= [0;0;0;0];

Q= [1   0    0    0    0;
    0    1   0    0    0;
    0    0    1    0    0;
    0    0    0    1    0;
    0    0    0    0    1]

R= [1]
[K, S, E] = lqr(A, B, Q, R)
```

Appendix-V

%% This program produces LQR control gains for Rayleigh beam model with single Rayleigh beam element using non-identity **Q** matrix

```
clc;
clear all;
A= [-1.37693 0 -13.4025 -1.30808 -0.65404;0 -14444.4 -3420.59 0 0;
-0.688463 1854.72 -180.493 -0.65404 -1.30808;
526.316 0 0 0 0;
0 0 10245.9 0 0];
B= [0;1;0;0;0];
C= [526.316 0 0 0 0;0 0 10245.9 0 0;
0 0 10245.9 0 0;
0 0 445389 0 0];
D= [0;0;0;0];

Q= [1   0     0     0     0;
    0     1    0     0     0;
    0     0     1     0     0;
    0     0     0     2.5     0;
    0     0     0     0     0.001]

R= [1]
[K, S, E] = lqr(A, B, Q, R)
```

Appendix-VI

%% This program produces LQR control gains for lumped parameter model with single Rayleigh beam element using non-identity **Q** matrix

```
clc;
clear all;
Ks= 1.3000;
Jeq= 9.76*10^(-5);
Js=0.0038274;
Req=0.01500;
Rm=2.6000;
kt=0.0077;
km=0.0077;
Kg=70;
eta_g=0.9000;
eta_m=0.6900;

%% State Space Representation
% The state space representation is shown
A=[0 0 1 0
  0 0 0 1
  0 Ks/Jeq -Req/Jeq 0
```

```
   0 -Ks*(Jeq+Js)/Jeq/Js Req/Jeq 0];
B= [0
      0
    1/Jeq
   -1/Jeq];
eig (A)
C= [1 0 0 0
     0 1 0 0]
 D= [0 0]'

 %% Actuator dyanmics added to the state space model
 % This part adds the motor dynamics given in Eq. (3.9) to the state space
 % model of the flexible manipulator
Ao = A;
Bo = B;
B = eta_g*Kg*eta_m*kt/Rm*Bo
A(3,3) = Ao(3,3) - Bo(3)*eta_g*Kg^2*eta_m*kt*km/Rm
A(4,3) = Ao(4,3) - Bo(4)*eta_g*Kg^2*eta_m*kt*km/Rm
Q= [ 150 0 0 0;
       0   1   0 0;
       0   0   1 0;
       0   0   0 3];
 R= [1];
 [K, S, E] = lqr (A, B, Q, R)
```

Thesis_Ebin_New

by Tarun Kumar Bera

Submission date: 14-Jul-2019 02:05PM (UTC+0530)
Submission ID: 442868756
File name: Thesis_Turnitin.docx (177.5K)
Word count: 22686
Character count: 112349

Thesis_Ebin_New

ORIGINALITY REPORT

7%	2%	3%	5%
SIMILARITY INDEX	INTERNET SOURCES	PUBLICATIONS	STUDENT PAPERS

PRIMARY SOURCES

1	Rochdi Merzouki, Arun Kumar Samantaray, Pushparaj Mani Pathak, Belkacem Ould Bouamama. "Intelligent Mechatronic Systems", Springer Nature, 2013 Publication	1%
2	realtyconnection.homesandland.com Internet Source	<1%
3	Submitted to Liverpool John Moores University Student Paper	<1%
4	Submitted to University of Sheffield Student Paper	<1%
5	Wolfgang Borutzky. "Bond Graph Methodology", Springer Nature, 2010 Publication	<1%
6	www.docstoc.com Internet Source	<1%
7	Submitted to iGroup Student Paper	<1%
	Submitted to IIT Delhi	

8	Student Paper	<1%
9	Submitted to International Islamic University Malaysia Student Paper	<1%
10	O. A. Bauchau. "Flexible Multibody Dynamics", Springer Science and Business Media LLC, 2011 Publication	<1%
11	Corvi, A.. "A preliminary approach to composite beam design using FEM analysis", Composite Structures, 1990 Publication	<1%
12	G. Surya Kiran, Amit Kumar, Pushparaj M. Pathak, N. Sukavanam. "Trajectory control of flexible space robot", 2008 IEEE International Conference on Mechatronics and Automation, 2008 Publication	<1%
13	"Trends in Intelligent Robotics, Automation, and Manufacturing", Springer Nature, 2012 Publication	<1%
14	data.ijmrs.com Internet Source	<1%
15	Submitted to VIT University Student Paper	<1%

16	Submitted to Cranfield University Student Paper	<1%
17	Submitted to Middle East Technical University Student Paper	<1%
18	Submitted to Jawaharlal Nehru Technological University Student Paper	<1%
19	Submitted to University of Surrey Student Paper	<1%
20	Submitted to University of Leicester Student Paper	<1%
21	Submitted to University of the West Indies Student Paper	<1%
22	www.slideshare.net Internet Source	<1%
23	Submitted to University of Huddersfield Student Paper	<1%
24	Submitted to Queen Mary and Westfield College Student Paper	<1%
25	Ling, Yun, Wei Lu, Changcheng Wu, Aiguo Song, and Chao Feng. "A novel rigid–flexible link combined lunar sampler and its basic dynamics and control", Aerospace Science and Technology, 2014. Publication	<1%

26	Submitted to University of Salford Student Paper	<1%
27	etd.ncsi.iisc.ernet.in Internet Source	<1%
28	Yun Ling, Wei Lu, Changcheng Wu, Aiguo Song, Chao Feng. "A novel rigid–flexible link combined lunar sampler and its basic dynamics and control", Aerospace Science and Technology, 2014 Publication	<1%
29	Submitted to Universiti Kebangsaan Malaysia Student Paper	<1%
30	Submitted to Universiti Teknologi Malaysia Student Paper	<1%
31	Giancarlo Genta. "Introduction to the Mechanics of Space Robots", Springer Nature, 2012 Publication	<1%
32	Submitted to University of Leeds Student Paper	<1%
33	Submitted to North West University Student Paper	<1%
34	Submitted to University of Aberdeen Student Paper	<1%
35	Dong-Soo Kwon, Wayne J. Book. "A Time-	<1%

	Domain Inverse Dynamic Tracking Control of a Single-Link Flexible Manipulator", Journal of Dynamic Systems, Measurement, and Control, 1994 Publication	
36	Submitted to Singapore International School Student Paper	<1%
37	www.cityandguilds.com Internet Source	<1%
38	Inman. "Control of Vibrations", Vibration with Control, 06/06/2006 Publication	<1%
39	Submitted to University of Southern California Student Paper	<1%
40	Submitted to Nottingham Trent University Student Paper	<1%
41	Submitted to Cranfield University Student Paper	<1%
42	Submitted to Technische Universiteit Delft Student Paper	<1%
43	Submitted to University of Johannsburg Student Paper	<1%
44	Submitted to The University of Manchester Student Paper	<1%

45	Submitted to Queensland University of Technology Student Paper	<1%
46	orca.cf.ac.uk Internet Source	<1%
47	T. Hitendra Sarma. "Speeding-Up the K-Means Clustering Method: A Prototype Based Approach", Lecture Notes in Computer Science, 2009 Publication	<1%
48	Submitted to University of Technology, Sydney Student Paper	<1%
49	Submitted to Indian Institute of Technology, Madras Student Paper	<1%
50	Submitted to Higher Education Commission Pakistan Student Paper	<1%
51	W. Blesser. "Nonlinear control with input preshaping for flexible-link manipulators", Fifth International Conference on Advanced Robotics Robots in Unstructured Environments, 1991 Publication	<1%
52	Submitted to University of Wollongong Student Paper	<1%

53	repository.ntu.edu.sg Internet Source	<1%
54	Ai Qun Liu. "Lateral Series Switches", MEMS Reference Shelf, 2010 Publication	<1%
55	Submitted to University of Birmingham Student Paper	<1%
56	Submitted to British University In Dubai Student Paper	<1%

Exclude quotes	On	Exclude matches	< 10 words
Exclude bibliography	On		